eman ta zabal zazu

Universidad del País Vasco
Euskal Herriko Unibertsitatea

KIMIKA ZIENTZIEN FAKULTATEA

FACULTAD DE CIENCIAS QUÍMICAS

Universidad del País Vasco/Euskal Herriko Unibertsitatea/ University of the Basque Country

Faculty of Chemistry

Degree in Chemistry

GRADU AMAIERAKO LANA

Novel redox active porous polymers to use as cathode in batteries

Author: Olatz Muñoz Ancisar

Supervisors: Haritz Sardon
Nerea Casado

Donostia-San Sebastián, July of 2018

GIPUZKOAKO CAMPUSA
CAMPUS DE GIPUZKOA
Pº. Manuel de Lardizabal, 3
20018 DONOSTIA-SAN SEBASTIAN
GIPUZKOA

ABSTRACT

Currently, several organic materials and polymers are under investigation as cathode materials for lithium batteries, for example: organic carbonyl compounds, conductive polymers, radical polymers or organosulfur compounds. Recently, redox-active Conjugated Microporous Polymers (CMPs) have emerged as potential electrode materials for energy storage devices. The aim of this work was to synthesize novel redox-active CMPs through Sonogashira cross-coupling reaction starting from tri- or tetra- functional monomers and different redox-active dibromine monomers. These monomers have different redox activity and therefore we envisioned that their redox properties would be different. First, the synthesis of the monomers was carried out followed by their characterization by ^{1}H and ^{13}C NMR, ATR-FTIR, mass spectrometry and elemental analysis. We found that the synthesis of the tri- and tetra- functional monomers was more favorable starting from iodide monomers than from bromine monomers.

Afterwards, the obtained monomers were employed for making porous polymers using Sonogashira reaction. The porous polymers were characterized by solid ^{13}C NMR, FTIR, BET, TGA and elemental analysis. Furthermore, the electrochemical properties of the monomers and polymers were studied through cyclic voltammetries. With this analysis the effect of the redox activity of each monomer after the polymerization was seen and it was possible to compare the redox activity of the different CMPs. The synthesized CMPs have shown potential as cathode materials, but still more studies are needed to confirm the electrochemical properties of these materials.

LABURPENA

Azken aldian, zenbait polimero eta material organiko aztertuak izaten ari dira litiozko baterietan katodo bezala erabiltzeko. Adibidez: karbonilodun konposatu organikoak, polimero eroankorrak, polimero erradikalak edo konposatu organosulfuroak. Duela gutxi, erredox aktiboak diren polimero mikroporoso konjugatuek (CMP), energia biltegiratzeko gailuetan elektrodo bezala erabiltzeko material bezala garrantzi handia hartu dute. Lan honen helburu nagusia erredox aktiboak diren CMP berriak sintetizatzea eta haien propietateak aztertzea da. Horretarako, CMP hauek *Sonogashira cross-coupling* erreakzioaren bidez sintetizatu dira, tri- edo tetra-funtzionalak diren monomeroetatik eta erredox aktiboak diren dibromo monomero ezberdinetatik abiatuz. Monomero hauen erredox aktibitatea ezberdina denez, suposatu da haien erredox propietateak ere ezberdinak izango direla. Hasteko, monomero hauen sintesiak egin dira eta jarraian karakterizatuak izan dira ^{1}H eta ^{13}C EMN, ATR-FTIR, masa espektrometria eta analisis elementala teknikak erabiliz. Gainera, ikusi da monomero ti- eta tetra- funtzionalen sintesia ioduro monomeroetatik abiatuz hobesten dela, bromuroetatik abiatu ordez.

Ondoren, monomero hauek erabili dira polimero porotsuak lortzeko *Sonogashira* erreakzioaren bidez. Polimero porotsu hauen karakterizazioa egin da ondorengo karakterizazio metodoak jarraituz: ^{13}C EMR, FTIR, BET, TGA eta analisis elementala. Honetaz gain, monomeroen eta polimeroen propietate elektrokimikoak boltametria ziklikoen bidez aztertu dira. Analisi honen bitartez polimerizazioaren ondoren monomero bakoitzaren erredox aktibitateak duen efektua ikusi da eta CMP desberdinen erredox aktibitatea konparatu da. Analisi guzti hauek sintetizatutako CMP ak katodoetarako material erabilgarriak izan daitezkeela erakutsi dute. Hala ere, material hauen propietate elektrokimikoak ezagutzeko beharrezkoa da azterketa gehiago egitea.

INDEX

1. INTRODUCTION

1.1 REDOX POLYMERS FOR ENERGY STORAGE DEVICES

Now-a-days, rechargeable batteries play a very important role in power source for portable consumer electronics, tools and electric vehicles [1]. Lithium ion batteries (LIBs) are one of the most popular energy storage devices because of their high energy density and cyclability [1,2-5]. These batteries are based on inorganic materials such as lithium metal oxides or phosphates. However, these inorganic materials come from mineral sources so they may run out and are generally toxic [6]. In order to deal with this problem, organic cathode materials including polymers have been studied and they have shown promising results for LIBs due to their high energy densities, environmental friendliness, structural diversity and controllability, and resource renewability [1,2,7,8].

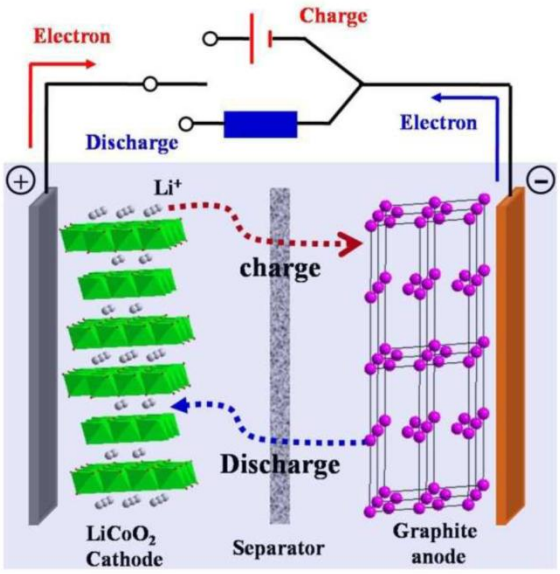

Figure 1: Schematic illustration of a LIB based on inorganic materials

Polymers can play different functions in an electrode of a battery. An electrode is based principally in a redox-active material, a binder and a conducting carbon. Until now the principal function of the polymers in the batteries has been as an inactive-material: such as binder where one of the most used is poly(vinylene fluoride) (PVDF).

Also they have been investigated to use as conducting additive to substitute the carbon. But in the last years, polymers have been studied as redox-active materials to replace the inorganic redox materials in the electrodes [6].

Polymers with redox properties are those with the ability of changing their electrochemical properties with the oxidation state due to the loss or gain of electrons. The IUPAC definition for these polymers is the following one: polymers containing groups that can be reversibly reduced or oxidized. The redox process can be given in a polymer main chain (example 1 and 2 of **figure 2**) or on side-groups (example 3 and 4 of **figure 2**). This depends on the nature of the polymer backbone, if it is conjugated or non-conjugated, and the presence or absence of spatially localized redox groups [9]. Redox polymers can have organic or inorganic redox centers; however, in this work we focus on organic materials.

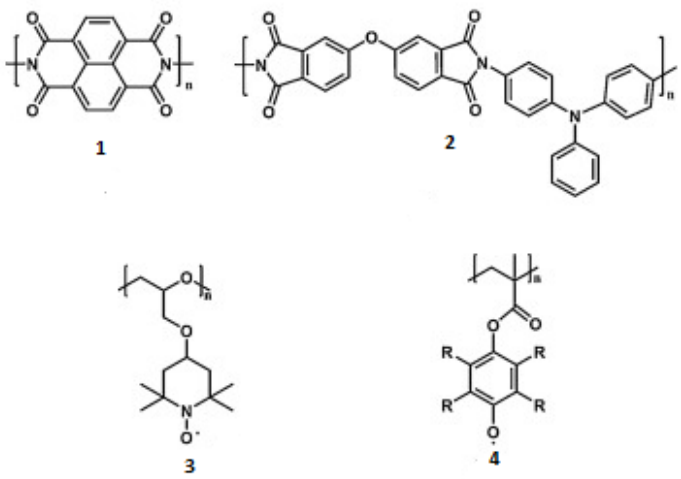

Figure 2: Examples of redox polymers

The redox properties of the polymers can be affected by intrinsic factors to the polymer chemical structure such as the nature and localization of the redox center, conjugation of the backbone or between redox centers and the ionic or conductivity properties of the polymer [9, 10]. But also can be affected by external factors like the

conditions of the measurements such as film thickness, kinetic processes, formulation of the electrode when conductive carbon and binders are added, nature of electrolyte and type of electrochemical cell and working and reference electrodes. Besides, at the time of the preparation of the electrode several issues must be taken into account like electric conduction in the electrode, capability of charge transfer at the electrode-polymer interface, diffusion towards the different electrolytes or optimal contents of the active material in the electrolyte [9, 11, 12].

1.2 POROUS POLYMERS

In the last years, porous materials have gained a great interest in different fields, because their pores and cavities can accommodate different types of molecules making them useful for different applications [13].

These materials can be totally inorganic materials (f.e. zeolites) [13, 14, 15], hybrid materials formed by an organic part and an inorganic part (MOFs, Metal Organic Frameworks) [13,16,17] and totally organic materials (POPs, Porous Organic Polymers) [13, 18, 19]. According to the IUPAC classification these materials can be divided in different groups depending on the size of their pores: macroporous materials with pores bigger than 50 nm, mesoporous materials with pores between 2 and 50 nm and microporous materials with pores smaller than 2 nm [13, 20]. Generally, the microporous materials have a very high specific surface (>1000 m^2 g^{-1}), mesoporous materials have lower specific surface and the macroporous materials have a very low specific surface (<50 m^2 g^{-1}). These parameters are obtained through the measurements of gas adsorption and are calculated using the Brunauer-Emmett-Teller (BET) theory [13, 21].

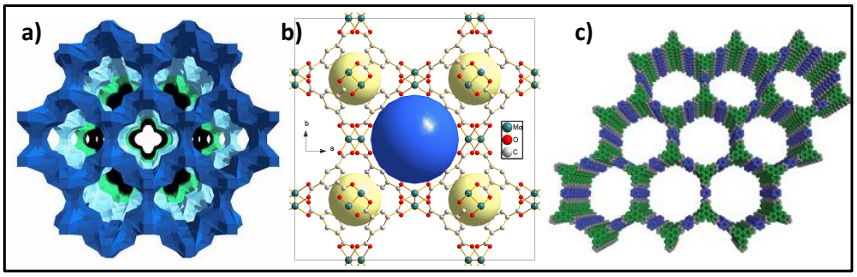

Figure 3: Structure of a) zeolite b) MOP and c) POP

In this project we focus on organic materials so the synthesized materials were POPs. These polymers present chemical structures with difficulties for package between them, and it is why porous systems are obtained in the synthesis. For the stability of these pores it is necessary to use monomers with low mobility like aromatic monomers. Most of the POPs have some grade of micro, meso and macro porosity and it is too difficult to obtain a homogeneous material respecting to the pore size. Also, most of the POPs are amorphous with a disordered structure and with high variety of the pore sizes. The most known synthetic POPs are the PIMs (Polymers of Intrinsic Microporosity) [13, 22], COFs (Covalent Organic Frameworks) [13, 23], HCPs Hypercrosslinked Polymers) [13, 24] and CMPs (Conjugated Microporous Polymers) [13, 25]. CMPs are porous polymers with an amorphous nature. In this project different CMPs were synthesized through a **Sonogashira cross-coupling** reaction between aromatic halides and aromatic alkynes catalyzed by palladium and copper [26].

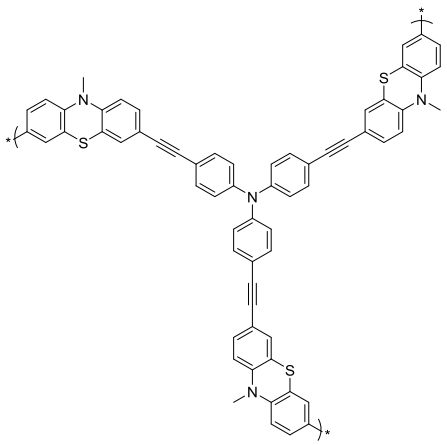

Figure 4: Example of a synthesized CMP

Sonogashira cross-coupling reaction consist in the cross coupling of aryl or vinyl halides with terminal alkynes to generate conjugated enynes arylalkynes. The reaction is performed in the presence of a palladium (0) catalyst, copper (I) cocatalyst and an imine base.

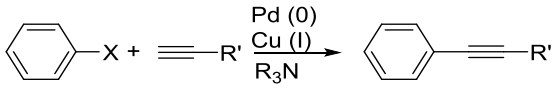

Scheme 1: General scheme of Sonogashira cross-coupling reaction for aryl halide. X= I, Br, Cl or OTf and R'=aryl, hetaryl, alkenyl, alkyl or SiR_3

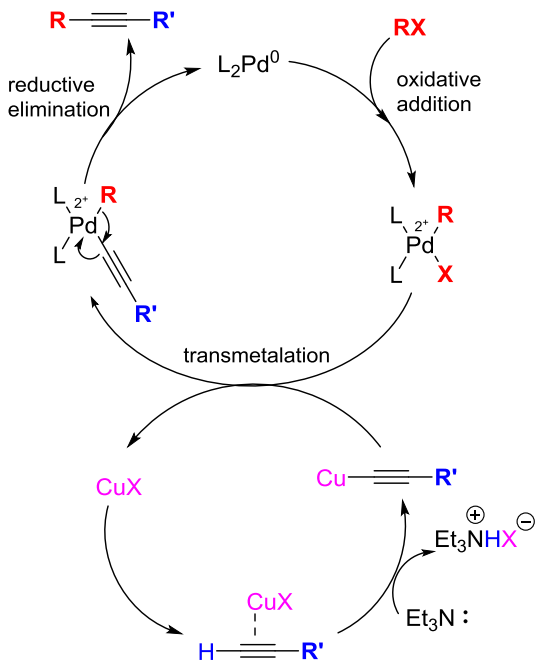

Scheme 2: General scheme of the mechanism of Sonogashira cross-coupling reaction

The mechanism of this reaction is based in a palladium cycle and a copper cycle. The reaction begins with the oxidative addition of the organohalide to the Pd (0) which reacts producing the Pd (II) complex. At the same time, in the presence of the base an organocopper reagent is formed from the terminal alkyne and the copper catalyst. The copper acetylide reacts in a transmetallation with the Pd (II) complex replacing the halide on the palladium complex and regenerating the copper halide. Finally, a reductive elimination gives the final coupled product and regenerates the palladium (0) catalyst [27].

1.3 REDOX POROUS POLYMERS FOR BATTERIES

Redox-active Conjugated Microporous Polymers have intrinsic advantages such as a high degree of π-conjunction, high specific surface area, diversity and flexibility in the molecular design, high chemical and thermal stability and insolubility in most solvents [1, 28]. Because of these advantages CMPs have shown great potential in some applications such as gas absorption [1, 29, 30], light emitting [1, 31, 32], energy storage [1, 33-38] and heterogeneous catalysis [1, 39-42]. These materials show a high specific surface area that provides abundant active sites for storage reactions and a microporous structure that is beneficial for the transport of electrons and ions [28]. Besides, high surface area of these materials allows for improved contact area with the electrolyte, more surface sites available for reversible reactions with Li^+ and shorter Li^+ diffusion pathway [1, 43-46].

C.Zhang et al. have employed different CMPs (SPTPA, YPTPA and OPTPA) as cathode materials for LIBs and have studied their electrochemical properties. The three polymers possess the same repeating triphenylamine (TPA) units and they combine high surface area with these redox-active TPA units. The results of this study show that increasing the surface area of polymer cathodes by interweaving the redox-active units into microporous polymer skeleton is an efficient way to develop advanced polymer cathode materials with outstanding electrochemical performances. Besides, it was demonstrated that the porous polymer skeleton makes very efficient utilization of the redox-active units for the energy storage and power supply since the high surface area and porous structure nature of the polymers facilitate the access of the electrolyte ions to the redox-active TPA units [1].

To sum up, different studies have demonstrated the enormous potential of CMPs as green, sustainable, flexible and high-performance electrode materials for next generation energy storage devices, especially for the fast charge-discharge cathode materials of lithium ion batteries (LIBs) [1, 28].

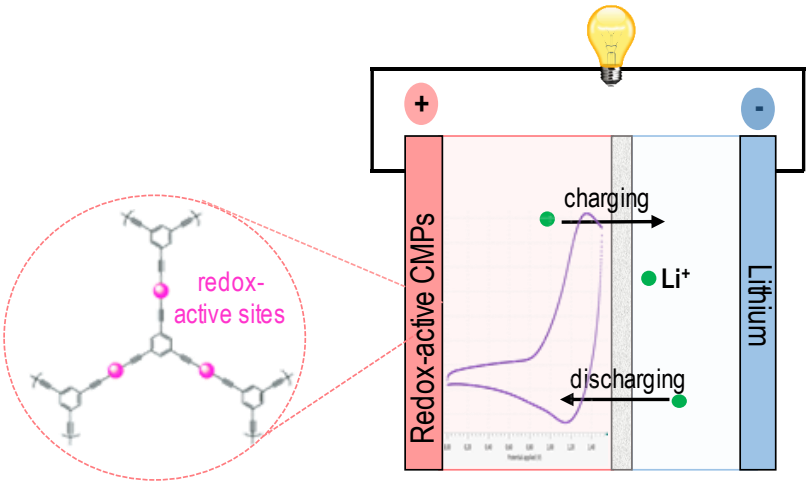

Figure 5: Schematic illustration of Lithium-Organic battery with redox active CMP cathode

2. OBJECTIVES

The main objective of this project was to synthesize new redox-active Conjugated Microporous Polymers and to analyze their properties. CMPs have emerged as potential materials for energy storage devices due to their advantageous intrinsic properties such as low solubility in comparison to small organic molecules or linear polymers. Furthermore, the redox-active sites in these porous frameworks are easily accessible by lithium ion during the charge-discharge process due to the high surface area and pore structure leading to high rate capability, which make them very attractive as cathode materials for batteries.

These compounds were synthesized according the following scheme:

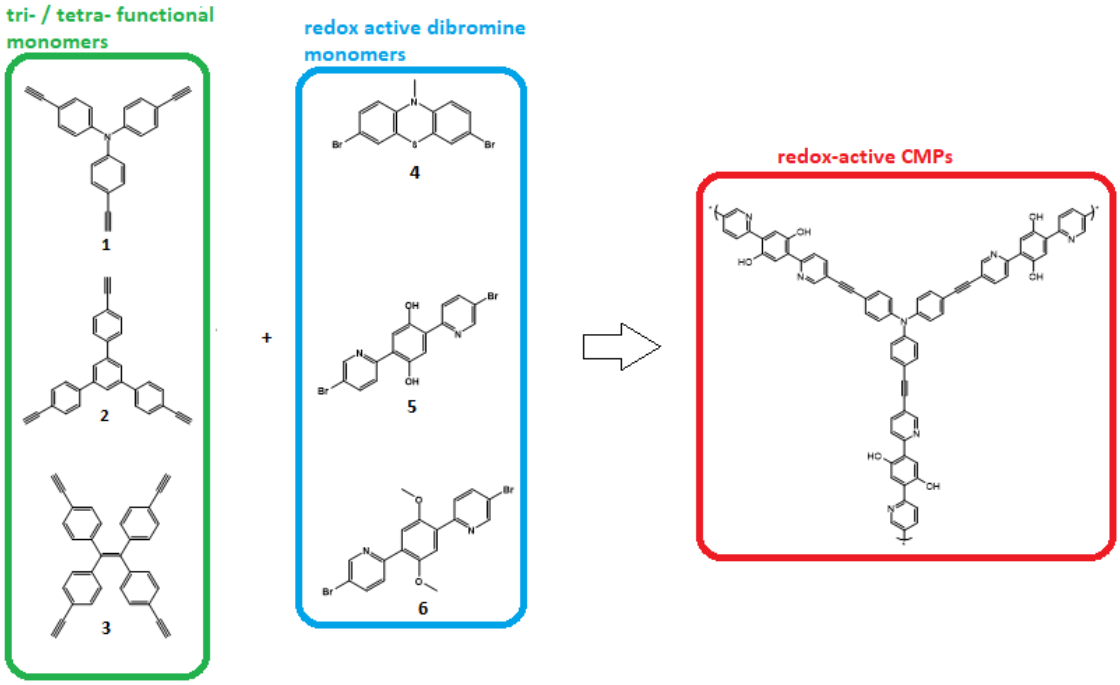

Scheme 3: General representation of the objective of the project.

On one hand we have three different tri-/tetra-functional monomers with different interesting properties. In the molecule **1** the nitrogen gives the redox-activity to the monomer whereas in molecules **2** and **3** the conjugation of the aromaticity through the aromatic ring (**2**) or the double bond (**3**) can provide electronic conduction through

the polymer. On the other hand we have three dibromine monomers with different redox activity. The syntheses of the CMPs were performed combining one monomer of the first group with other of the second group through Sonogashira cross-coupling reaction. Studying the structural and electrochemical properties of the obtained monomers and polymers it might be possible to see which monomers (tri-/tetra-functional ones or dibromine ones) have more effect in the redox activity of the CMPs. We wanted to use different monomers of each group to compare the specific surface and the electrochemical properties of the obtained CMPs and decide which monomers could be the best ones to synthesize a CMP with the best properties to use as cathode material in batteries.

After the synthesis of each monomer and polymer they were characterized by different characterization methods to confirm that the reactions occurred successfully. Used characterization methods were ^{1}H and ^{13}C NMR, ATR-FTIR, mass spectrometry and elemental analysis for monomers and ^{13}C NMR, FTIR, BET, TGA and elemental analysis for polymers.

To sum up, the main goal of this work is the synthesis and characterization of these materials, as well as to put in practice all the skills acquired during the Chemistry degree.

3. RESULTS AND DISCUSSION

3.1 SYNTHESIS OF MONOMERS

First of all, the tri-/tetra- functional monomers and dibromine monomers were synthesized starting from commercial monomers. Most of the syntheses were described previously and some of them were adapted from other synthetic procedures.

3.1.1 Synthesis of tri- and tetra- functional monomers

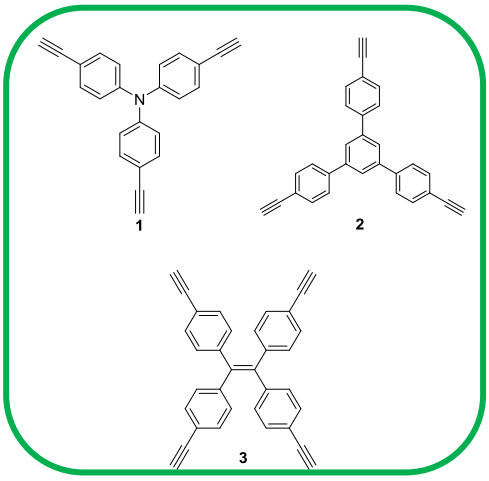

Scheme 1: tri- and tetra- functional monomers

The synthesis of the molecule **1** was based on previous reports and it is given in two synthetic steps starting from a commercial monomer (**Scheme 5**) [47]. First, the replacement of the iodide was given by Sonogashira cross-coupling reaction. Due to the high reactivity of the iodide the replacement was given for all iodides and it was not obtained any mixture of products. Then, the reaction was continued with the deprotection of the trimethylsilylalkynyl compound by potassium carbonate obtaining the final product with a yield of 57 %.

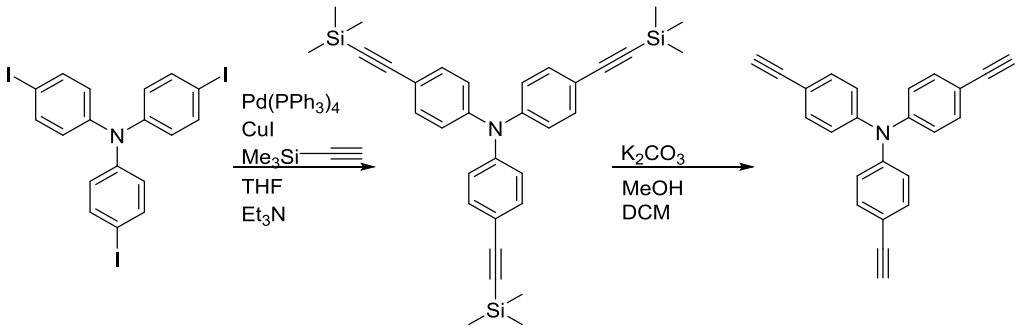

Scheme 2: Simple scheme of the synthesis of molecule 1

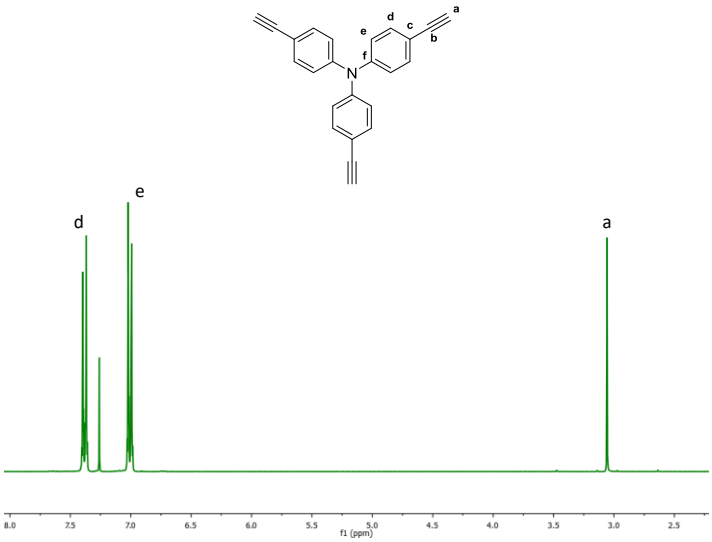

Figure 6: ^{1}H NMR spectrum of the monomer 1

The syntheses of the molecules **2** and **3** were tried following two different synthetic procedures, but the final products were not obtained, as it is shown below.

First synthetic way was based in previous reports and it is given in three synthetic steps for both monomers. In the synthesis of the tri-functional monomer (**2**), in the first reaction the product was obtained by cyclic self-condensation of three molecules of aryl ketones [48].

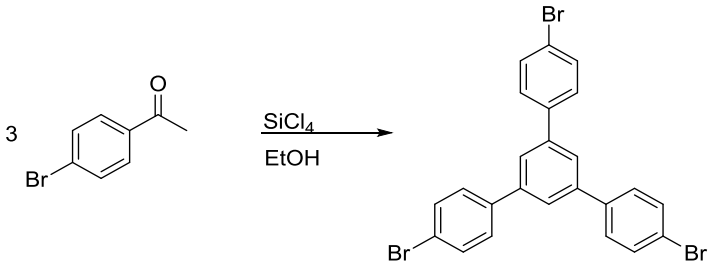

Scheme 3: First reaction for the synthesis of monomer 2 in the first synthetic way

For the tetra-functional one (**3**) instead, the first reaction is given trough McMurry reaction, where two ketones were coupled to an alkene in presence of Ti (IV) chloride and zinc as a reducing agent [49]. First, a single electron was transferred to the carbonyl group forming a diol compound. Then, the alkene was obtained through the deoxygenation of the diol with low-valent titanium which was reduced by the zinc [50].

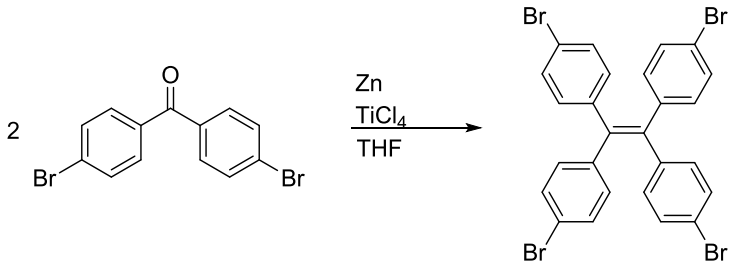

Scheme 4: First reaction for the synthesis of monomer 3 in the first synthetic way

The second step of both syntheses consists in a Sonogashira cross-coupling reaction where bromines were supposed to be replaced by trimethylsilylacetylene [51]. In this case, it was seen in the ^{1}H NMR that we obtained a mixture of mono- , di- , tri- and tetra- substituted products and it was so difficult to separate them by chromatographic column. So it was not possible to continue the synthesis to obtain the final pure products.

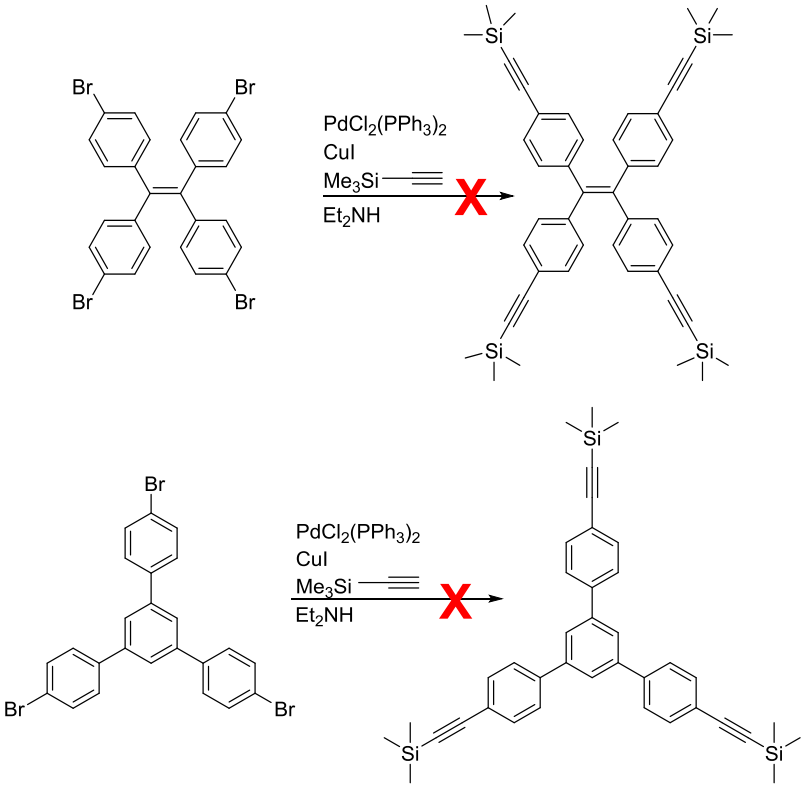

Scheme 5: Second reaction for the synthesis of the monomers 2 and 3 in the first synthetic way

Therefore, a second synthetic way was used for the syntheses of monomers **2** and **3**. This was based in described procedures and it is given in three synthetic steps too [51]. But in this case the procedure starts with the Sonogashira cross-coupling reaction and it continues with McMurry and the cyclic self-condensation. This time, the Sonogashira cross-coupling reaction works well and it might be because less bromine had to be replaced.

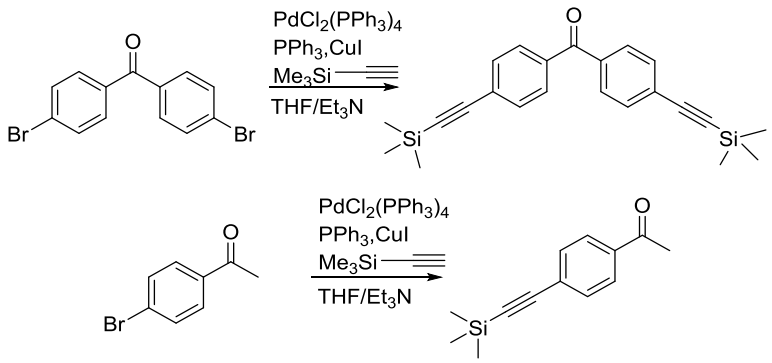

Scheme 6: First reaction for the synthesis of the monomers 2 and 3 in the second synthetic way

Once that the bromines were replaced by Sonogashira cross-coupling, McMurry reaction and the cyclic self-condensation were applied in order to obtain the tetra- and tri- functional compounds. Unfortunately in the ^{1}H-NMR spectra it was seen that the desired products were not obtained.

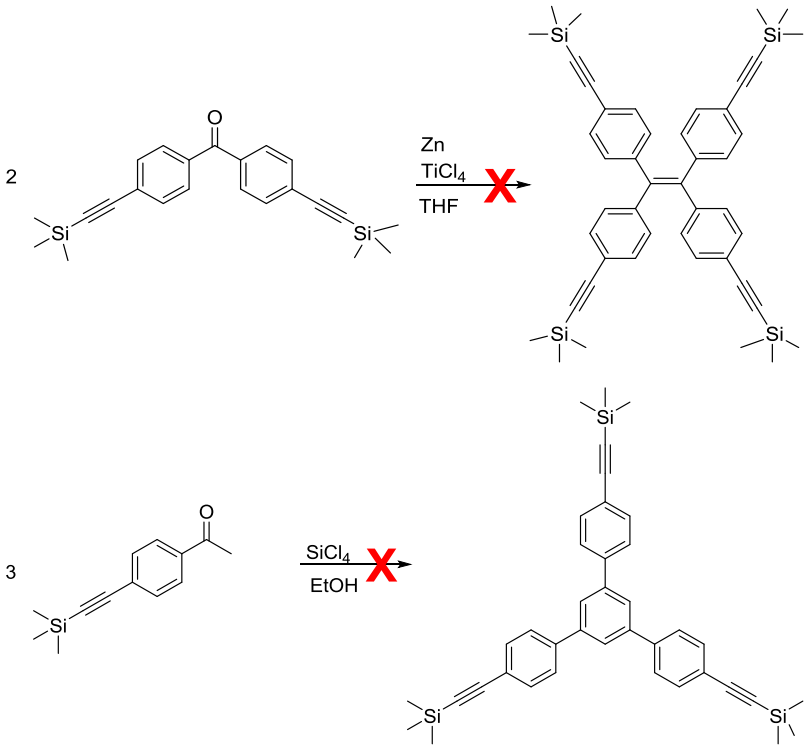

Scheme 7: Second reactions for the synthesis of monomers 2 and 3 in the second synthetic way

Every reaction of these syntheses was done in anhydrous and anaerobic conditions to avoid any side reaction and the degradation of the catalysts.

For the synthesis of these monomers the main reaction is the named **Sonogashira cross-coupling** reaction. This reaction is used to form triple carbon-carbon bonds. It consist in the cross coupling of aryl or vinyl halides with terminal alkynes to generate conjugated enynes arylalkynes. The reaction is performed in the presence of a palladium (0) catalyst, copper (I) cocatalyst and an imine base.

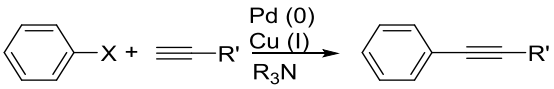

Scheme 8: General scheme of Sonogashira cross-coupling reaction for aryl halide. X= I, Br, Cl or OTf and R'=aryl, hetaryl, alkenyl, alkyl or SiR_3

For the synthesis of molecules **1**, **2** and **3**; X= I or Br, R'= $SiMe_3$, $Pd(PPh_3)_4$ or $PdCl_2(PPh_3)_2$ as Pd (0) catalyst, CuI as Cu (I) cocatalyst and Et_3N or Et_2NH as imine base were used.

As it has been said before, at the beginning the intention was to synthesize three tri- or tetra- functional monomers and even I have tried to synthesize them all, I have only got the first one.

3.1.2 Synthesis of dibromine monomers

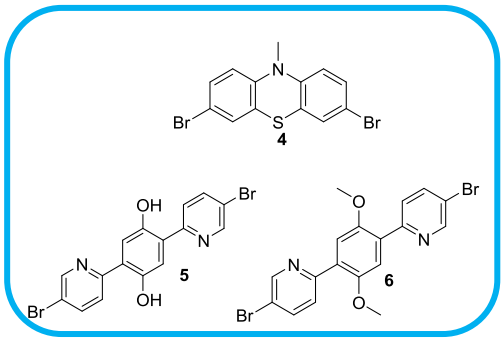

Scheme 9: dibromine monomers

Synthesis of 3,7-dibromo-10-methyl-10H-phenothiazine

The synthesis of the molecule **4** was based in previous reports and it is given in one step starting from a commercial product [52]. The reaction was given by bromination reaction in presence of the N-bromosuccinimide with a yield of 32 %.

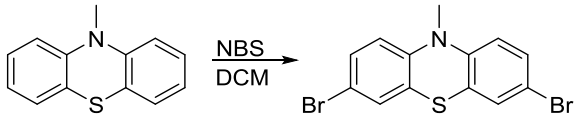

Scheme 10: General scheme of the synthesis of monomer 4

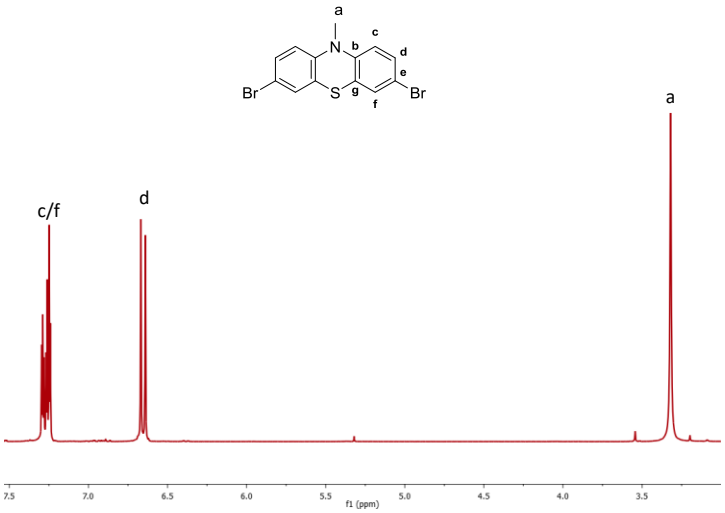

Figure 7: ^{1}H NMR spectrum of the monomer 4

Synthesis of 6,6'-(2,5-dimethoxy-1,4-phenylene)bis(3-bromopyridine) and 2,5-bis(5-bromopyridin-2-yl)benzene-1,4-diol

The synthesis of the monomer **6** was given in two synthetic steps in which the first one was previously described and was based in previous reports [53]. The diboronic acid was obtained through a halide/metal exchange using n-BuLi as a base and triethyl borate as electrophilic reagent in THF solution with a yield of 26 %.

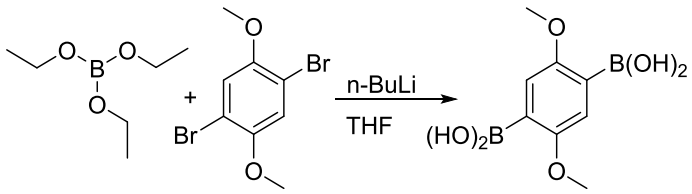

Scheme 11: First reaction for the synthesis of monomer 6

The monomer **6** was never synthesized before, so the synthesis of this diboronic monomer was adapted from other reports [54]. It was obtained by Suzuki coupling of

the diboronic acid with the dibromopiridyne using Pd (0) as catalyst and sodium carbonate as a base.

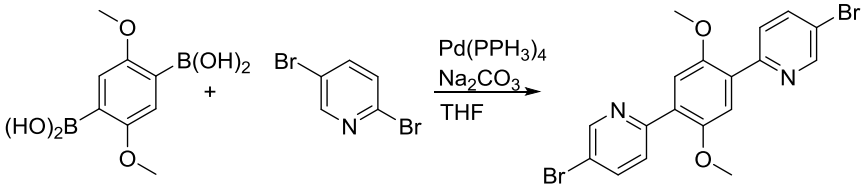

Scheme 12: Second reaction for the synthesis of monomer 6

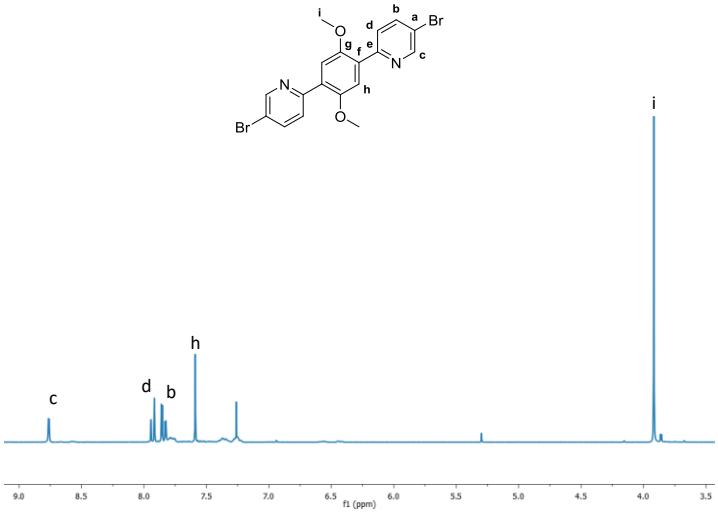

Figure 8: ^{1}H NMR spectrum of the monomer 6

Finally, the monomer **5** was synthesized by the deprotection of the methoxy group in presence of the aluminum chloride through Meerwein-Ponndorf-Verley reduction obtaining the diol compound.

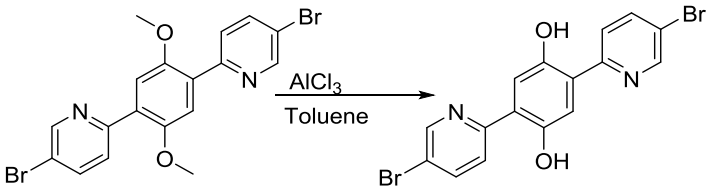

Scheme 13: Third reaction for the synthesis of the monomer 5

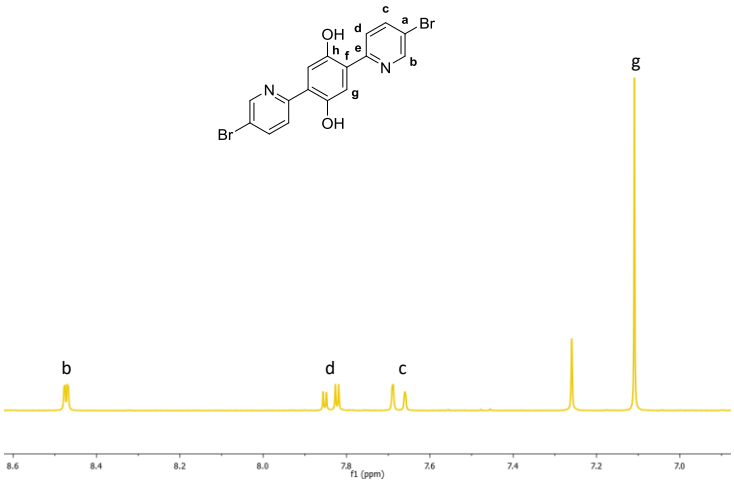

Figure 9: ^{1}H NMR spectrum of the monomer 5

3.2 SYNTHESIS OF POLYMERS

The synthesis of the polymers was performed through Sonogashira cross-coupling reaction using $Pd(PPh_3)_4$ as Pd (0) catalyst and CuI as Cu (I) cocatalyst [55]. As in the synthesis of monomers, this reaction was done in anhydrous and anaerobic conditions. In the reactions, the synthesized tri-functional monomer reacts with synthesized three dibromine monomers obtaining three different CMPs.

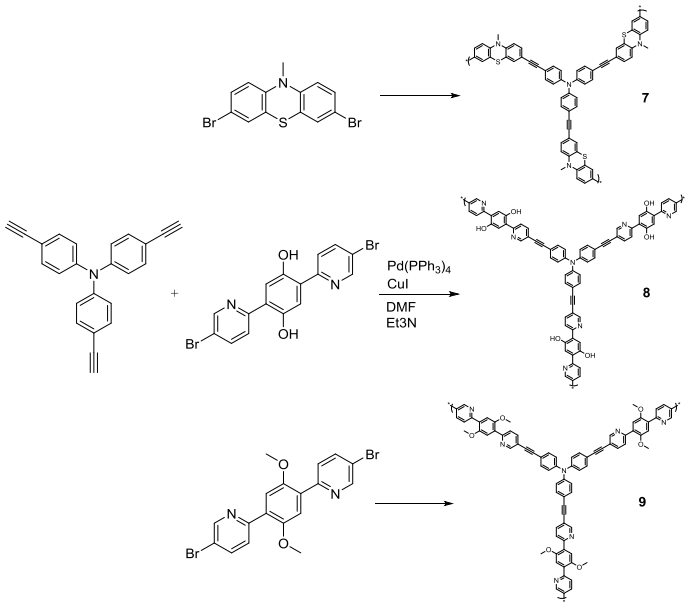

Scheme 14: General scheme of the synthesis of the CMPs

After some essays of this reaction the conditions that are shown in the following table were selected as the best ones. After the reaction, the purification of the polymers was done by Soxhlet extraction and they were dried in a lyophilizer.

Table 1: Selected conditions for the synthesis of the CMPs

Monomer 1	Monomer 4, 5 or 6	$Pd(PPh_3)_4$	CuI	DMF	Et_3N	Time
1 eq.	1 eq.	0.08 eq.	0.15 eq.	109 eq.	30 eq.	5 days

In order to optimize this reaction different conditions were varied to obtain higher surface area. The reaction time was varied from 3 to 5 days, the catalyst content and monomer concentration were also varied in order to decrease the polymerization rate (0,04 eq. of tetrakis(triphenylphosphine)palladium(0) and 0,09 eq. of copper iodide). Finally in order to get the highest surface area the purification method was also studied. Thus, the obtained polymers were washed with different solvents: acetonitrile, water, acetone, chloroform and diethyl ether (50 ml of each one). And finally, they was dried using different conditions and temperatures (**table 2**).

Table 2: Results of the texture properties for synthesized polymers

Molecule	Changed conditions	Degasification conditions	BET surface area ($m^2\ g^{-1}$)
7	5 days, dried at 250 °C	120 °C, 10 h.	419,9
7	5 days, lyophilized	120 °C, 10 h.	619,9
7	5 days, lyophilized	200 °C, 10 h.	559,7
7	3 days, less catalyst eq.	120 °C, 10 h.	3,025
8	5 days, lyophilized	120 °C, 10 h.	464
9	5 days, dried at 120 °C	120 °C, 10 h.	**1023**

In this kind of materials, conjugated microporous polymers, the surface area is usually in majority microporous and in a lower percentage mesoporous, and the specific surface area is normally around 500/900 $m^2 g^{-1}$. First of all, the results of the obtained materials were compared when the time of the reaction and the equivalents of the catalyst were changed. It was seen that when the reaction time was decrease to 3 days and less catalyst amount was used, the specific surface area was much lower than in any other conditions. So these conditions were automatically discarded. Then, the method used for drying the polymer **7** was compared and it was seen that higher BET surface area was obtained when the material was dried in the lyophilizer. It might be due to the high temperature of 250 °C, because the polymer **9** was also dried by heating but with lower temperature (120 °C) and actually it was the material with the best surface area. Finally, the method of the degasification was studied for the same polymer (**7**) and the results showed that with higher temperature the surface area was worse, once again.

Summarizing the best conditions to obtain highest surface area are the following ones: 5 days for the reaction; 0,8 eq. of $Pd(PPh_3)_4$ and 0,15 eq. of CuI; dry in a liophilizer or heating without exceeding 120 °C and degasification at 120 °C for 10 h.

3.3 CHARACTERIZATION OF POLYMERS

Besides, with the Barrett-Joyner-Halenda (BJH) method the average of the pore size was determined for each material. A pore is considered micro-pore when its size is less than 2 nm, meso-pore when the size is between 2 and 50 nm and macro-pore when the size is bigger than 50 nm. As we can see in the **table 3**, the average pore size of every polymer is less than 10 nm and for the polymers **7** and **9** is almost 2 nm. It means that even these materials have the presence of mesopores mostly they are microporous so they can be considerate as CMPs.

Furthermore, whit the BET method it was possible to measure the total specific surface area and the micropourus surface area so with these two data it was possible to confirm that the surface area of these materials were in majority microporous.

Table 3: Data of the proportion of the micro- and meso-pore area of the synthesized CMPs

Molecule	Total surface area ($m^2 g^{-1}$)	Micropore area ($m^2 g^{-1}$)	Mesopore area ($m^2 g^{-1}$)	Total pore volume ($cm^3 g^{-1}$)	Pore size equivalent (nm)
7	616,9	336,7	283,2	0,538	3,5
8	464	175,7	288,3	0,915	7,9
9	1023	657,5	365,5	0,687	2,7

To sum up, depending on the results it has to be said that the material **9** might be the CMP with best texture properties that makes this material very interesting to use as cathode material in batteries.

In spite of these good results, must be mentioned that this information was obtained from an adsorption-desorption isotherm in which the desorption line is different in the isotherm (**figure 10**). This result suggest that most probably the pore size may be affected due to the presence of some residual monomer or solvent inside the pores, or because the pores were not totally rigid and they suffered some deformation.

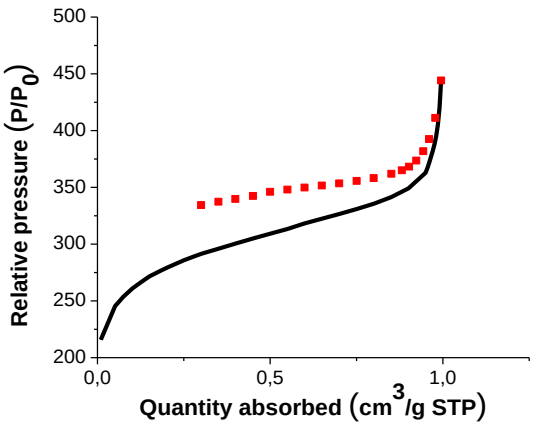

Figure 10: Absorption-desorption isotherme of the polymer 9

The thermal properties of the polymers were analyzed by TGA method. It was necessary to do the measurements under oxidant atmosphere (air) to see a complete degradation of these polymers. As we can see in **figure 11** the degradation of the polymers starts at very high temperatures and the residue after the measurements under nitrogen atmosphere is much higher than under an oxidant atmosphere.

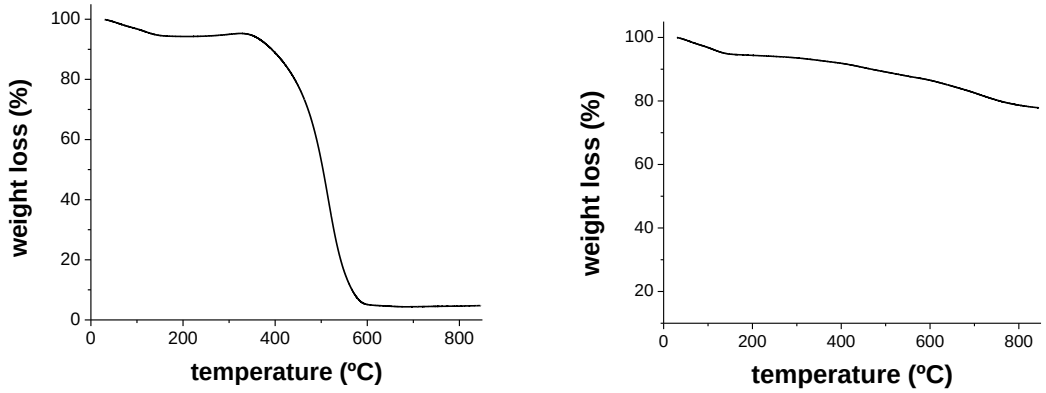

Figure 11: TGA analysis of a CMP in oxidant atmosphere and in nitrogen atmosphere

In the figure below (**figure 12**) it is shown the TGA analysis of the three CMPs. As can be observed the degradation of these materials starts at high temperatures, around 380 °C and they are not completely degraded until almost 600 °C, so they can be considered as stable materials. Despite the analysis of the three polymers is too similar, the degradation of the polymer **9** starts and finish a little bit earlier than the other ones.

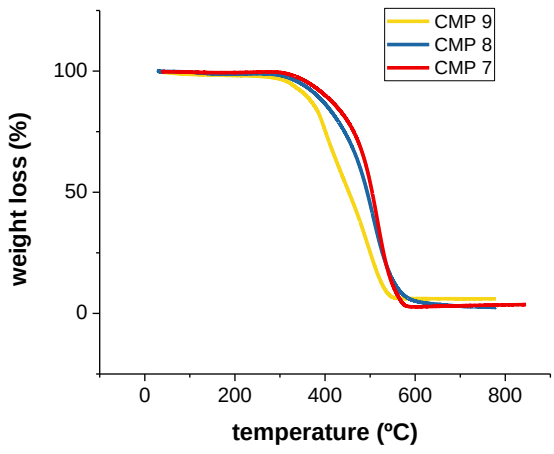

Figure 12: TGA analysis of the CMPs under oxidant atmosphere

Fourier transform infrared spectroscopy was used to analyze the structural properties of the polymers, and to confirm that the desired product was obtained after polymerization. This technique gives qualitative information of the functional groups of the sample, so the signals should be similar to the monomers' ones.

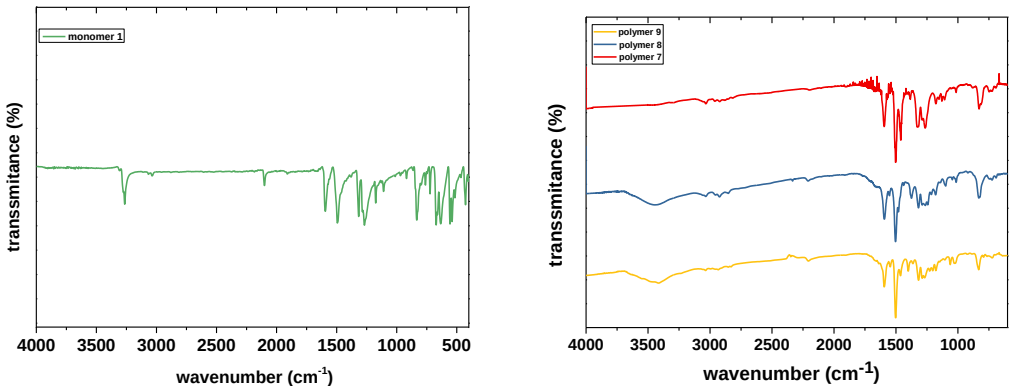

Figure 13: Infrared spectra for monomer 1 and polymers

Looking at the spectra of the monomer **1** in the **figure 13** it can be seen the peak of the C-H of the triple bond at 3264 cm^{-1} and the peak of the C-C triple bond at 2104 cm^{-1}. However, if we look at the spectra of the polymers we can see that the peak of the C-H is disappeared after the polymerization. That confirms that the polymers were successfully obtained.

If we look at the spectra of the polymers in the **figure 13**, we can see that some peaks are the same for all the polymers but also that there are some differences between them. The peaks attributed to the aromatic rings appear at around 1595 cm^{-1}, 1500 cm^{-1} and between 1460 and 1480 cm^{-1} in the spectra of three polymers. Also there is a peak at around 1320 cm^{-1} in the three spectra and it correspond to the stretching of C-N bond. However, we can see a peak at 1373 cm^{-1} for the polymer **8** and at 1400 cm^{-1} for polymer **9** that are not seen in the polymer **7**. This peak corresponds to the C-O bond (Ph-OH in the case of the polymer **8** and Ph-O-CH_3 in the case of polymer **9**). Apart from that, in the polymers **8** and **9** there is a peak at 3500 cm^{-1}, it is the typical peak of the OH. This peak was supposed to appear in the polymer **8** only but it appears

in the polymer **9** too. It might be because of the presence of residual water or because the methoxy group starts deprotecting.

^{13}C-NMR spectroscopy was performed in a solid state due to the insolubility of these materials. Because of the structure of these polymers it is too difficult to see good spectra and to assign a signal to each carbon. In **figure 14** there are represented the spectra of the three CMPs. In the spectrum of the polymer **8** all the signals appear between 100 and 150 ppm, which correspond to the aromatic carbons. In the case of the polymers **7** and **9** apart from the signals corresponding to the aromatics carbon (between 100 and 150 ppm), there can be seen a signal at 55 ppm for the polymer **9** corresponding to the carbon of the methoxy group; and a signal at 90 ppm for the polymer **7** corresponding to the carbon of the methyl group of the amine.

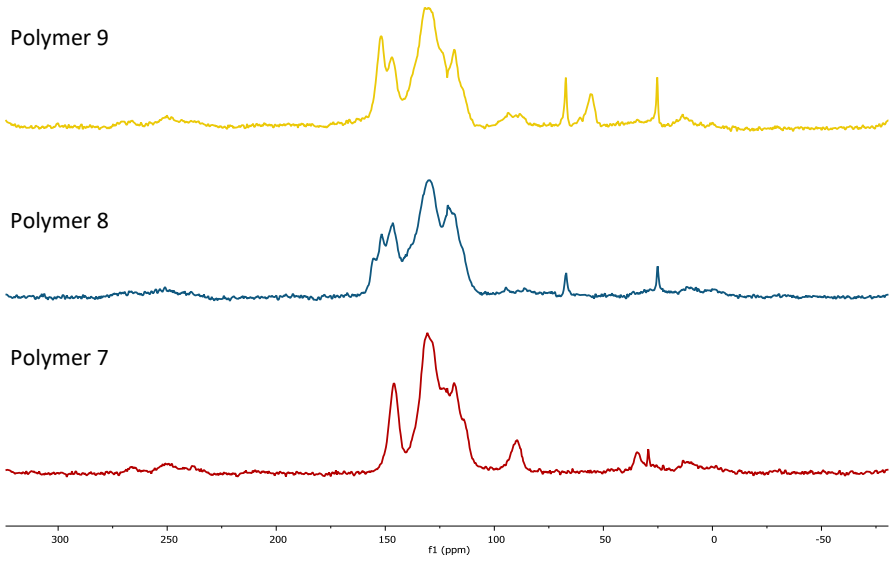

Figure 14: representation of the ^{13}CNMR spectra of the CMPs

Finally, the electrochemical properties of these materials were analyzed by cyclic voltammetry, and the results were studied and compared with the monomers' electrochemical properties. First, cyclic voltammetry measurements of the monomers were done in a small cell using glassy carbon as working electrode. Different

electrolytes were used for these measurements in order to determine in which electrolyte the oxidation-reduction process would be favored. In case of the monomer **4** the measurements were done in organic electrolytes as 0,1 M LiTFSi/ACN and 0,1 M $LiClO_4$/ACN. For both electrolytes the redox activity of this monomer was the same. The measurements of the monomer **5** besides of doing them in organic electrolytes they were also performed in aqueous electrolyte (0.1 M $HClO_4$). Aqueous electrolyte favors the redox reaction of this monomer, as the protons of the alcohol groups are involved in the redox reaction, as can be seen in **scheme 18**. At the beginning, there was not expected any redox-activity for monomer **6** due to its structure, but after the measurements it was seen that it was active in both aqueous and organic electrolytes, this could be again because the methoxy group is not stable and starts deprotecting. Finally, the monomer **1** was analyzed in every electrolyte, but in this case the redox-activity was seen only in organic electrolytes. As it can be seen in the representation of the measurements bellow, every monomer was redox-active, reversible and stable.

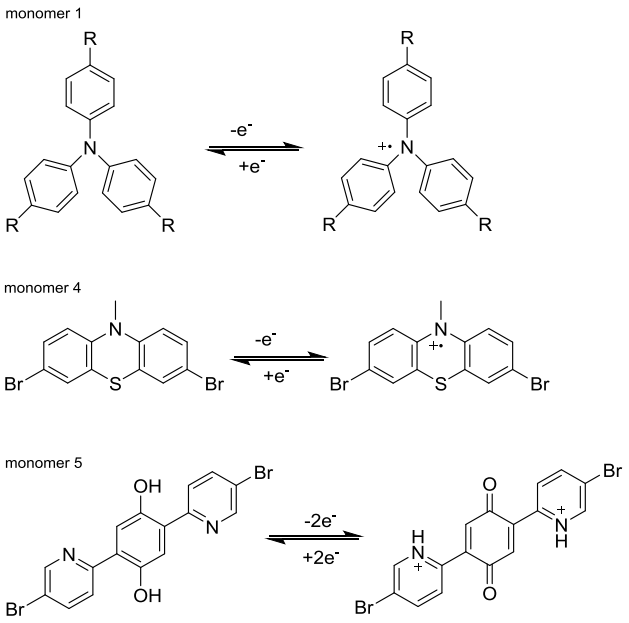

Scheme 15: Representation of the redox reactions of the monomers

After the measurements of the monomers the polymers were analyzed. The measurements of the polymer **7** were done in organic electrolyte and of the polymers **8** and **9** in aqueous electrolyte.

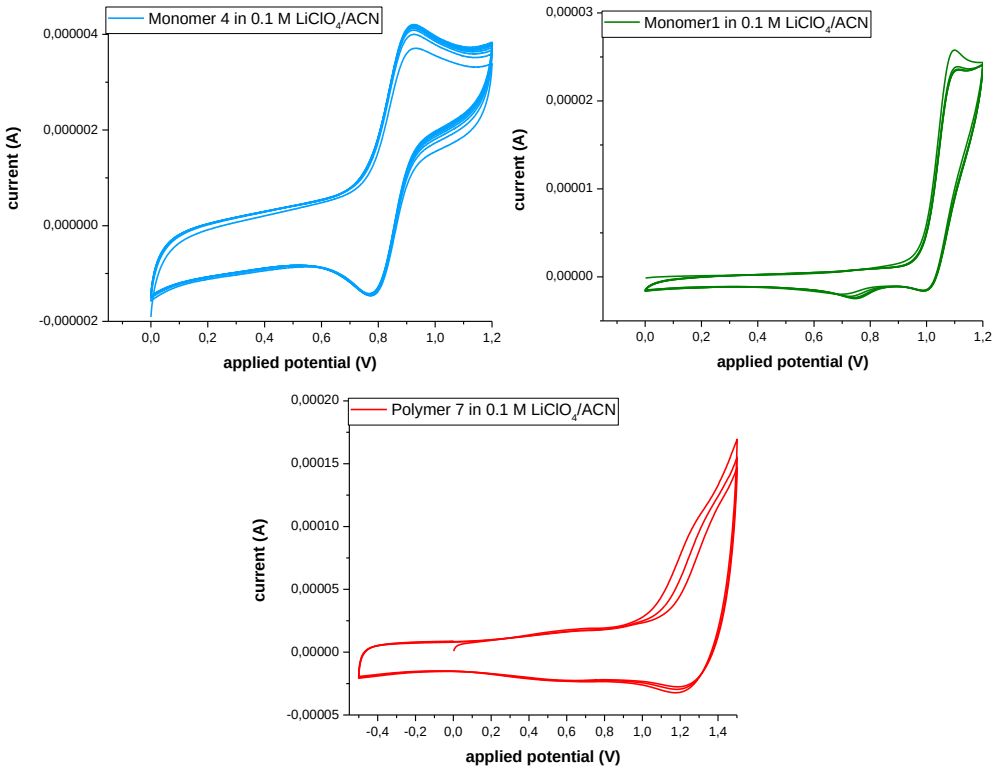

Figure 15: Representation of the cyclic voltammetry of the monomer 4, monomer 1 and polymer 7 in 0.1 M $LiCO_4$/ACN electrolyte

As the **figure 15** shows, both monomers are redox-active, stable and reversible in this electrolyte. The oxidation and reduction peaks are seen clearly. The oxidation of the monomer **4** is given around of 0,9 V and the reduction around 0,8 V. In the cyclic voltammetry of the polymer only one peak of oxidation and one peak of reduction were seen. That means that the oxidation and reduction of both monomers were given at the same time in the polymer. The oxidation is given at 1,2 V and the reduction at 1,3 V. In the representation of the polymer can be seen that the peaks are not as clear as the peaks of the monomers. This might be because the monomers were dissolved in the electrolyte while the polymers were studied in film form, difficulting the clear definition of the peaks. Nevertheless, we can confirm that this material is redox-active.

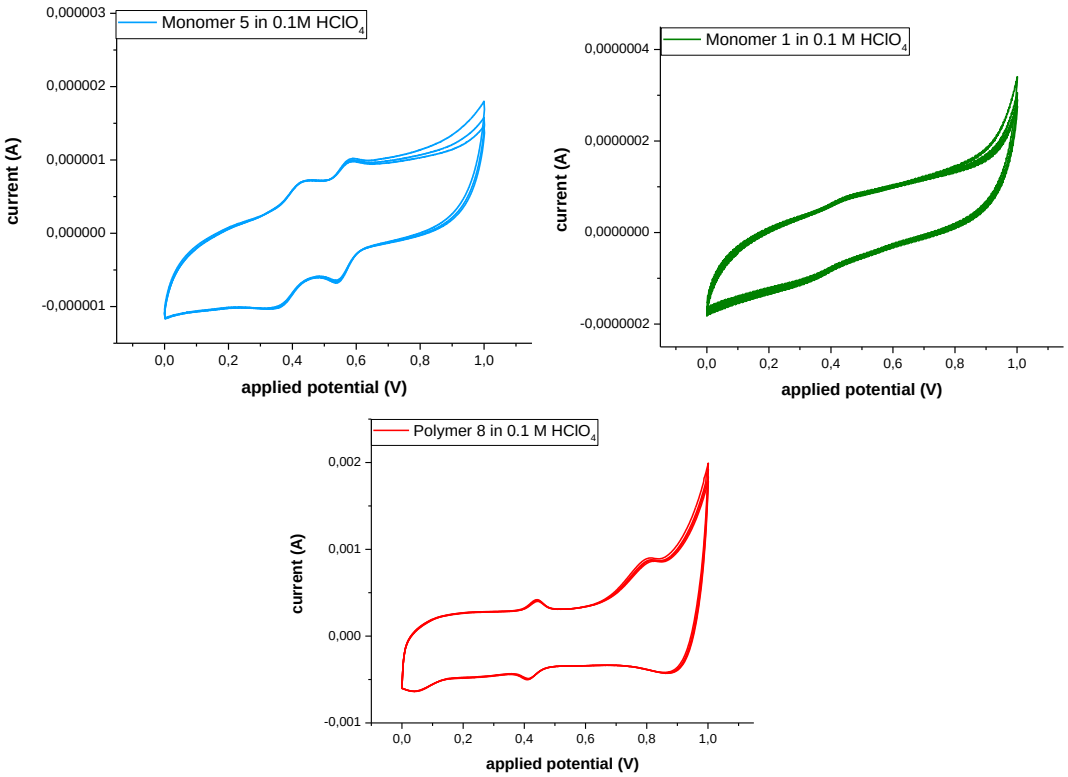

Figure 16: Representation of the cyclic voltammetry of the monomer 5, monomer 1 and polymer 8 in 0.1 M $HClO_4$ electrolyte

In the **figure 16** it can be seen that the monomer **5** was redox-active in this aqueous electrolyte and that two redox processes were given. In the first one the oxidation was given at 0,45 V and the reduction at 0,37 V. In the second one the oxidation was given at almost 0,6 V and the reduction at 0,55 V. This can be because the redox reaction of the two alcohol groups does not occur at the same voltage. In the case of the monomer **1** instead, it was seen that it was not redox-active in aqueous electrolyte. If we look at the cyclic voltammetry of the polymer **8**, there can be seen two redox processes. First one was given around 0,4 V which is related to the redox process given through the monomer **5**. The second one was given around 0,85 V so it might be given through the monomer **1**. As it was seen, even the monomer **1** was not active in this electrolyte as free monomer, after the polymerization it became active. Despite the peaks of the redox process were not so pronounced, it was seen that this material also was redox-active, so it would be useful for applications with aqueous electrolytes, such as, aqueous batteries.

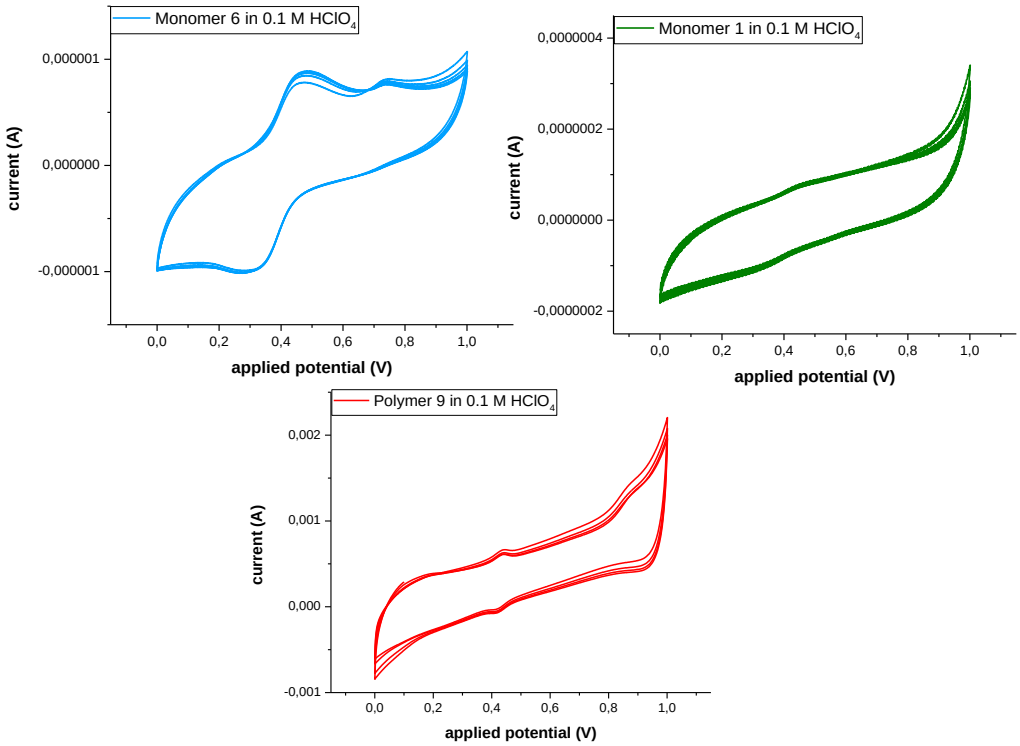

Figure 17: Representation of the cyclic voltammetry of the monomer 6, monomer 1 and polymer 9 in 0.1 M $HClO_4$ electrolyte

The results of the measurements of the polymer **9** and of the free monomers of this compound were very similar to the polymer **8**. The only difference is that in the monomer **6** one redox process is given, in which the oxidation is given at 0,45 V and the reduction at 0,35 V. The monomer **1** became active after the polymerization too but the redox process was given in higher potentials. The oxidation was given at 0,9 V and the reduction at 0,95 V. The redox process of the monomer **6** in the polymer was given exactly at the same potential than in the polymer **8**.

Finally, in order to study the stability of the redox processes of the polymers, cyclic voltammetry measurements were done in different scan ratios from 5 mV s^{-1} to 100 mV s^{-1}.

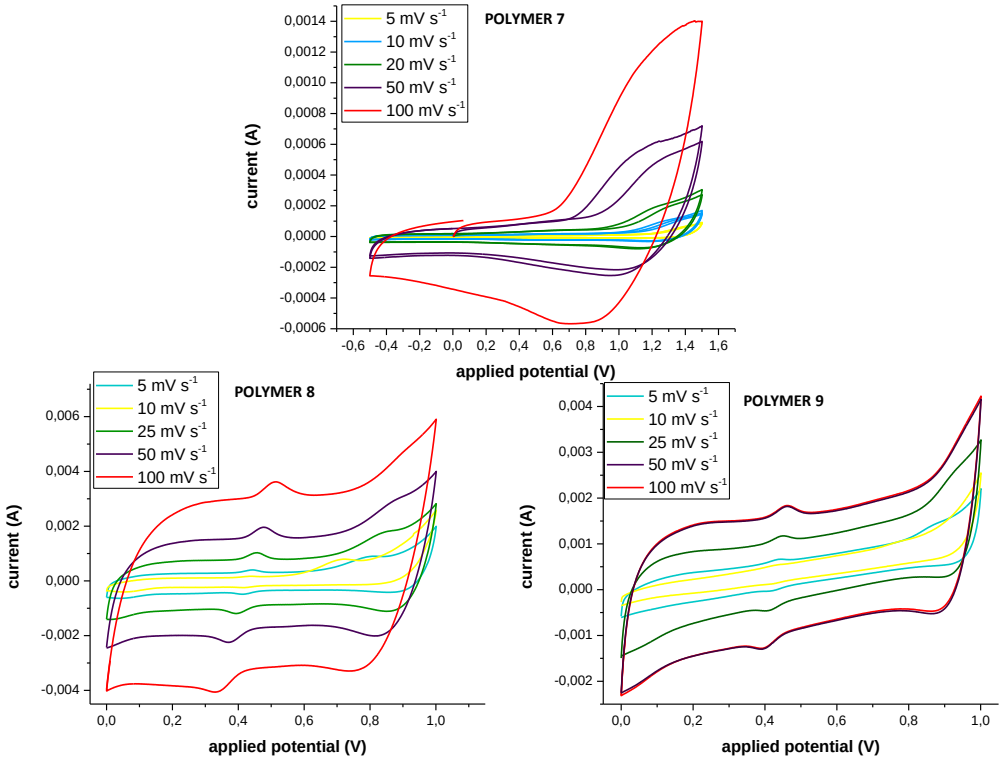

Figure 18: Representation of the cyclic voltammetry measurement of polymer 7, polymer 8 and polymer 9 in different scan rates

As **figure 18** shows, the current increases with the increment of the speed of the applied potential. But sometimes, with this increment of the speed of the applied potential the redox process may stop working or become more irreversible (bigger separation of oxidation and reduction potentials). In the case of polymer **7**, it can be seen that when the current was increasing, the redox peak separation was increasing. Therefore, this polymer could not probably be cycled at high current densities in batteries. In case of the polymers **8** and **9,** when the current increases with the increment of the speed, the potential of the redox peaks keep stable as with lower speed. Therefore, polymers **8** and **9** are appropriate to cycle at high current densities.

With all this information it was shown that the electrochemical properties of the polymers **8** and **9** were better than polymer **7**. It was seen that the redox process was better distinguished and was more stable at high rates in these polymers. This might be due to the higher pore size and BET surface area of these polymers. Even that, it

was seen that reversible redox processes were given in every polymers so it can be said that these materials are interesting to keep studying for energy storage device applications.

4. EXPERIMENTAL

4.1 REACTANTS AND SOLVENTS

The reactants and solvents were supplied by Sigma Aldrich, Fisher end Acros Organics and they were used without previous purification. The synthesized monomers were purified by silica gel column chromatography and for this silica gel (0,035-0,070 mm, 60 A) was used, acquired from Acros Organics. The solvents used as eluent were obtained from Scharlab and used without any purification.

4.2 CHARACTERIZATION METHODS

Obtained monomers and polymers were characterized by different methods. It has to be said that these polymers are insoluble solids due to their structure, and it makes them difficult to characterize completely.

4.2.1 Thermal properties

Thermogravimetric analysis (TGA)

With this method the degradation of the materials was studied by measuring the weight loss of the materials during the increment of the temperature in an oxidant atmosphere. A Q500 Thermogravimetric Anlayzer from TA Instruments was used for this analysis and the sample was heated from room temperature to 800/850 °C in a rate of 10 °C min^{-1} under a constant air flow of 60ml min^{-1}.

In this case it can't be used the differential scanning calorimetry (DSC) analysis to determine the rest of the thermal properties, due to the lack of mobility of the polymer's structure.

4.2.2 Structural properties

Fourier Transform Infrared spectroscopy (FTIR)

This technique has been used to see the conversion grade of the monomers and polymers after the reactions. In those spectra the functional groups of the compounds were seen and qualitatively determinated.

For the monomers the measurements were done by attenuated total reflection (ATR) whereas for the polymers KBr pills were prepared and the spectra were registered in a Nicolet Magna 6700 spectrometer at room temperature. In both cases the spectra were obtained by Fourier transform at absorption terms (cm^{-1}).

^{1}H and ^{13}C Nuclear Magnetic Resonance (NMR)

Monomer's spectra were realized at room temperature on Bruker Avance DPX 300 at 300 MHz of resonance frequency for ^{1}H-NMR and 100 MHz for ^{13}C-NMR using deuterated chloroform or deuterated dimethyl sulfoxide as solvent. The experimental conditions for the ^{1}H NMR were 10 mg of sample, 3 s acquisition time, 1 s delay time, 8.5 µs pulse, spectral width 5000 Hz and 32 scans. For the ^{13}C NMR 30 mg, inverse gated decoupled sequence, 3 s acquisition time, 4 s delay time, 5.5 µs pulse, spectral width 18,800 Hz and more than 10,000 scans.

As it's said, synthesized polymers are not soluble in any solvent, so the spectra were performed in solid state. The spectra of the solid polymers were performed in a Bruker Avance III 9.4 T at 100,64 MHz. The samples were introduced in a probe MAS/DVT of 4mm with rotors of ZrO at room temperature and they were rotated at 12 KHz. The spectrums were performed by cross polarization sequence (CPMAS). The experimental conditions were 6024 scans, 3,5 µs pulse, a contact time of 2,0 ms, recycling relay of 5 s, spinning rate 12000Hz and spectral width 30 KHz.

This technique can confirm in a qualitative way the final structure of the obtained product through the assignment of the different hydrogen or carbons. Due to the disordered structure of the polymers the assignment of these C peaks is not that clear.

Mass spectrometry

This technique was used to know the mass of the different monomers and to confirm their chemical structure. The analysis consisted in a chromatographic separation in an ultrahigh performance liquid chromatograph (UPLC, Acquity system from Waters Cromatografia S.A.) coupled to a high resolution mass spectrometer (Synapt G2 from Waters Cromatografia S.A., time of flight analyzer (TOF)) by an electrospray ionization source in positive mode (ESI+). High resolution mass data were acquired in SCAN mode, using a mass range 50–1200 u in resolution mode (FWHM ≈ 20,000) and a scan time of 0.1 s. The source temperature was set to 120 °C and the desolvation temperature to 350 °C. The capillary voltage was 0.7 kV and the cone voltage 15 V. Nitrogen was used as the desolvation and cone gas at flow rates of 600 L/h and 10 L/h, respectively. The samples were dissolved in the corresponding solvent and diluted in methanol at a concentration of 20 µg mL^{-1} for the analysis.

Elemental Analysis (EA)

In order to analyze the composition of the monomers and polymers the elemental analysis for C,H and N was done in a Euro EA 3000 (Eurovector, Italia). For the analysis 5 mg of the sample were placed in the auto-sampler and they were periodically tipped into a vertical quartz reactor heated at a temperature of 980 °C with a constant flow of helium stream. The combustion gas mixture was subjected to a process of oxidation and reduction where the resulting components were N_2, CO_2 and H_2O. These components were separated and detected by a thermo conductivity detector. The resulting signals were analyzed by Callidus® software which automatically provides the sample elemental composition report.

This analysis in polymer networks can be difficult to interpret because sometimes the percent of the pyrolyzed material is not 100%.

4.2.3 Textural properties

These properties were determinate by N_2 absorption and desorption varying the pressure at liquid nitrogen temperature. The experiments were performed in a Micromerities ASAP 2020 instrument. The samples were previously degassed for 10 h at 120 °C. These measurements generate the adsorption-desorption isotherms in which we can deduce the amount of absorbed N_2 on the tasted sample. This will determine the specific surface area, the pore volume and the pore size. The specific surface area is determinated by the Brunauer-Emmett-Teller (BET) method. The Barrett-Joyner-Halenda (BJH) method was used for determine the pore size distribution.

4.2.4 Electrochemical properties

The electrochemical properties of the monomers were measured in a three electrode cell with platinum wire as counter electrode, glassy carbon as working electrode and Ag/AgCl as reference electrode. 0,1 M $LiClO_4$ in acetonitrile solution, 0,1 M LiTFSI in acetonitrile solution or 0,1 M Bu_4NPF_6 in dichloromethane solution were used as electrolyte and for the measurement the monomers were dissolved in the electrolyte(1 mM monomer concentration). 0,1 M $HClO_4$ aqueous solution was used as electrolyte also for some monomers, but in this case these monomers were not soluble in there. A little amount of monomer was dissolved in dichloromethane and a small amount was deposited in the working electrode. The dichloromethane was evaporated and a thin layer of monomer was rested in the electrode, ready for the measurement.

In the case of polymers a mixture of 50 wt% polymer, 40 wt% Ketjenblack EC-600JD, AzkoNobel and 10 wt% PDVF in N-methyl-2-pyrrolidone (NMP) was prepared for the characterization. A three electrode cell was used with platinum plate as counter

electrode, modified glassy carbon as working electrode and Ag/AgCl as reference electrode. The slurry containing active material was uniformly casted over the current collector (glassy carbon electrode) and 0,1 M $HClO_4$ aqueous solution and 0,1 M $LiClO_4$ in acetonitrile solution were used as electrolyte for the characterization of the polymers.

In both cases the electrochemical characterization was performed on an Autolab PGSTAT204.

Cyclic voltammetry measurements were conducted at 50 mV s^{-1} for monomers and at different scan rates from 5 mV s^{-1} to 100 mV s^{-1} for polymers. These measurements were done to confirm the redox activity and the stability of the materials.

4.3 SYNTHESIS OF MONOMERS

a) 3,7-dibromo-10-methyl-10H-phenothiazine. 0,750 g of *10H*-phenothiazine (3,51 mmol) were added into a 100 ml flask and flushed with nitrogen to obtain an inert atmosphere. 15 ml of dichloromethane anhydrous were added and stirred until a colorless solution was obtained. The solution was cooled to 0 °C and 1,570 g N-bromosuccinimide (8,79 mmol, 2,5 eq.) were added in three portions, every 15 min each one. The color of the reaction became green. The reaction was warmed to room temperature and stirred overnight. The mixture of the reaction was diluted with distilled water (20 ml) and the crude product was extracted with dichloromethane (2 x 20 ml). The combined organic layers were dried with anhydrous magnesium sulfate. Then, magnesium sulfate was filtered and the solvents were removed in vacuum. The obtained crude product was a purple solid and it was purified

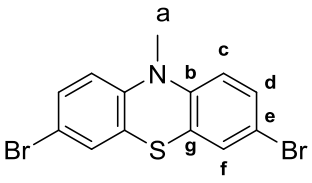

by silica gel column chromatography using hexane/dichloromethane (5:1) as eluent. Crystalline white solid was obtained (yield: 32 %).

- ^{1}HRMN (300 MHz, Chloroform-*d*) δ (ppm): 7,28 (m, 4H, H_c /H_f); 6,66 (d, *J* = 8,5 Hz, 2H, H_d); 3,32 (s, 3H, H_a).
- ^{13}CNMR (100 MHz, chloroform-*d*) δ (ppm): 144,74 (C, C_b); 130,43 (CH, C_d); 129,56 (CH, C_f); 125,00 (C, C_e); 115,45 (CH, C_c); 115,12 (C, C_g); 35,58 (CH_3, C_a).
- Calculated elemental analysis for $C_{13}H_9Br_2NS$: C 42,08; H 2,44; N 3,77 %.

  Obtained elemental analysis for $C_{13}H_9Br_2NS$: C 41,4; H 3,54; N 3,92 %.

b) Tris(4-((trimethylsilyl)ethynyl)phenyl)amine. 910 mg of tris(4-iodophenyl)amine

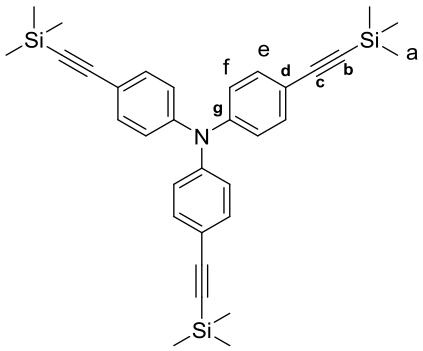

(1,46 mmol) were added to 29,2 ml of tetrahydrofuran and 11,7 ml of triethylamine solution into a 100 ml flask. The mixture was degassed with nitrogen for 1 h. Then, 41,8 mg of tetrakis(triphenylphosphine)palladium(0) (0,0862 mmol, 0,06 eq.) were added and the mixture was degassed 15 min more. 516 mg of trimethylsilylacethylene (5,27 mmol, 3,6 eq.) were added dropwise into the mixture. When the addition was finished 34,5 mg of copper iodide (0,18 mmol, 0,12 eq.) were added and the mixture was degassed for 30 min. Finally, the mixture was stirred for 24 h at room temperature. The mixture of the reaction was a black suspension and the solids were removed by filtration. The filtered phase was quenched with a solution of ammonium chloride and the crude product was extracted with dichloromethane (3 x 50 ml). The combined organic phases were dried with anhydrous sodium sulfate. The sodium sulfate was filtered and solvents were removed in vacuum. The obtained crude product was a yellow-brown solid and it was washed with an acid solution. 710 mg were obtained (yield: 91 %).

- ^{1}H NMR (300 MHz, Chloroform-*d*) δ (ppm): 7,34 (d, *J* = 8,8 Hz, 6H, H_f); 6,95 (d, *J* = 8,8 Hz, 6H, H_e); 0,24 (s, 27H, H_a).
- ^{13}CNMR (100 MHz, chloroform-*d*) δ (ppm): 146,93 (C, C_g); 133,31 (CH, C_e); 123,95 (CH, C_f); 117,95 (C, C_d); 105,00 (C, C_c); 94,11 (C, C_b); 0,17 (CH_3, C_a).
- MS (ESI, *m/z*) calculated for $C_{33}H_{39}NSi_3$: 533,2469 ; found: 533,2457

c) Tris(4-ethynylphenyl)amine. 650 mg of Tris(4-((trimethylsilyl)ethynyl)phenyl)amine (1,2 mmol) were added to a solution containing 16 ml of methanol and 16 ml of dichloromethane into a 100 ml flask. After the solution was completed 723,5 mg of potassium carbonate (5,24 mmol, 4,31 eq.) were added into the mixture and it was stirred at room temperature overnight. The mixture was poured into 30 ml of water and the crude product was extracted with dichloromethane (3 x 30 ml). The combined organic phases were dried with anhydrous sodium sulfate. The sodium sulfate was filtered and the solvents were removed in vacuum. The obtained crude product was purified by silica gel column chromatography using chloroform/petroleum ether as eluent. 244 mg of the product were obtained (yield: 63 %).

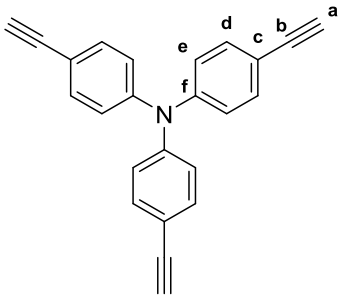

- ^{1}HRMN (300 MHz, Chloroform-*d*) δ (ppm): 7,38 (d, *J* = 8,7 Hz, 6H, H_d); 7,01 (d, *J* = 8,8 Hz, 6H, H_e); 3,06 (s, 3H, H_a).
- ^{13}CNMR (100 MHz, chloroform-*d*) δ (ppm): 147,18 (C, C_f); 133,52 (CH, C_d); 124,09 (CH, C_e); 117,02 (C, C_c); 83,56 (C, C_b); 77,16 (CH, C_a).
- Calculated elemental analysis for $C_{24}H_{15}N$: C 90,82; H 4,76; N 4,41 %. Obtained elemental analysis for $C_{24}H_{15}N$: C >85,00; H 5,41; N 4,75 %.

d) 4,4''-dibromo-5'-(4-bromophenyl)-1,1':3',1''-terphenyl. 5 g of 1-(4-bromophenyl)ethan-1-one (25,1 mmol) were added to 40 ml of absolute ethanol into a 250 ml flask. The mixture was cooled to 0 °C and 18,5 g of silicon tetrachloride (108,9 mmol, 4,34 eq.) were added dropwise. The mixture was warmed to room temperature and then refluxed for 24 h. During the reaction the mixture became yellow. After cooling the mixture to room temperature 50 ml of saturated ammonium chloride solution were added and it was stirred for 30 min. The obtained product was filtered and recrystallized from ethanol. At the end 4,44 g of white solid was obtained (yield: 98 %).

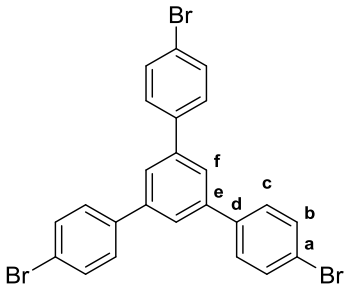

- ^{1}HRMN (300 MHz, Chloroform-*d*) δ (ppm): 7,69 (s, 3H, H_f); 7,61 (d, *J* = 8,6 Hz, 6H, H_b); 7,54 (d, *J* = 8,6 Hz, 6H, H_c).
- ^{13}CNMR (100 MHz, chloroform-*d*) δ (ppm): 141,65 (C, C_d); 139,75 (C, C_e); 132,18 (CH, C_c); 129,02 (CH, C_f); 125,11 (CH, C_b); 122,24 (C, C_a).

e) 1-(4-((trimethylsilyl)ethynyl)phenyl)ethan-1-one. 4 g of 1-(4-bromophenyl)ethan-1-one (20,11 mmol), 0,282 g of bis(triphenylphosphine)palladium(II) dichloride (0,402 mmol, 0,02 eq.), 0,316 g of triphenylphosphine (1,207 mmol, 0,06 eq.) and 0,153 g of copper iodide (0,804 mmol, 0,04 eq.) were added into a 250 ml flask. The flask was evacuated and flushed with nitrogen three times to obtain an inert atmosphere. In the meantime a solution of tetrahydrofuran/triethylamine (70 ml/ 70 ml) was degassed for 1h. The degassed solution was added to the flask with reactants. Then 2,963 g of trimethylsilylacethylene (30,165 mmol, 1,5 eq.) were added dropwise. The reaction was refluxed at 50 °C for 24h. A black solid was formed in the reaction and it was removed by filtration and washed with diethyl ether. Finally the solvents were removed in vacuum. The crude product was a brown liquid and it was purified by silica gel column

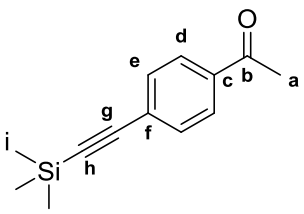

chromatography using hexane/ethyl acetate (100:1) as eluent. It were obtained 2,77 g of yellow liquid (yield: 64 %).

- ^{1}H NMR (300 MHz, Chloroform-*d*) δ (ppm): 7,88 (d, *J* = 8,6 Hz, 2H, H_d); 7,53 (d, *J* = 8,6 Hz, 2H, H_e); 2,59 (s, 3H, H_a); 0,26 (s, 9H, H_i).
- ^{13}CNMR (100 MHz, chloroform-*d*) δ (ppm): 197,39 (C, C_b); 136,49 (C, C_c); 132,18 (CH, C_e); 128,72 (CH, C_d); 128,07 (C, C_f); 104,13 (C, C_g); 98,21 (C, C_h); -0,05 (CH_3, C_i).
- MS (ESI, *m/z*) calculated for $C_{13}H_{16}OSi$: 217,1049 ; found: 217,1050

f) 1,1,2,2-tetrakis(4-bromophenyl)ethane. 5 g of bis(4-bromophenyl)methanone

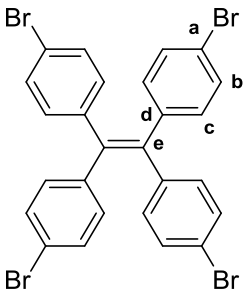

(14,7 mmol) and 2,29 g of Zn dust (35,29 mmol, 2.4 eq.) were added to 176 ml of tetrahydrofuran anhydorus into a 500 ml flask and it was flushed with nitrogen for 30 min. The solution was cooled to -78 °C and 3,38 g of titanium tetrachloride (17,64 mmol, 1,2 eq.) were added dropwise. The mixture was stirred at this temperature for 30 min and then it was warmed to room temperature. Finally it was refluxed at 70 °C overnight. The mixture of the reaction was diluted with water and the crude product was extracted with chloroform (3 x 50 ml). The combined organic phases were dried with anhydrous magnesium sulfate. The magnesium sulfate was filtered and solvents were removed in vacuum. Brown solid was obtained as a crude product and it was purified by silica gel column chromatography using hexane/dichloromethane (100:10) as eluent. At the end 2,95 g of white solid were obtained (yield: 62 %).

- ^{1}HRMN (300 MHz, Chloroform-*d*) δ (ppm): 7,26 (d, *J* = 8,6 Hz, 8H, H_b); 6,84 (d, *J* = 8,6 Hz, 8H, H_c).
- ^{13}CNMR (100 MHz, chloroform-*d*) δ (ppm): 141,62 (C, C_e); 139,76 (C, C_d); 132,88 (CH, C_b); 131,45 (CH, C_c); 121,43 (C, C_a).

g) (4-((trimethylsilyl)ethynyl)phenyl)methanone. 3 g of bis(4-bromophenyl)methanone (8,82 mmol), 0,248 g of bis(triphenylphosphine)palladium(II) dichloride (0,353 mmol, 0,04 eq.), 0,278 g of triphenylphosphine (1,058 mmol, 0,12 eq.) and 0,134 g of copper iodide (0,706 mmol, 0,08 eq.) were added into a 250 ml flask. The flask was evacuated and flushed with nitrogen three times to obtain an inert atmosphere. In the meantime a solution of tetrahydrofuran/triethylamine (44 ml/ 44 ml) was degassed for 1h. The degassed solution was added to the flask with reactants. Then 2,166 g of trimethylsilylacethylene (22,05 mmol, 2,5 eq.) were added dropwise. The reaction was refluxed at 50 °C for 24h. A black solid was formed in the reaction and it was removed by filtration and washed with diethyl ether. Finally the solvents were removed in vacuum. The crude product was purified by silica gel column chromatography using hexane/ethyl acetate (100:1) as eluent. At the end 3,07 g of white product were obtained (yield: 93 %)

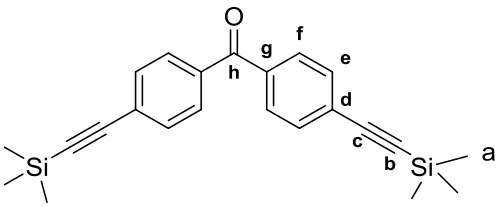

- ^{1}H NMR (300 MHz, Chloroform-*d*) δ (ppm): 7,71 (d, *J* = 8,6 Hz, 4H, H_f); 7,56 (d, *J* = 8,6 Hz, 4H, H_e); 0,27 (s, 18H, H_a).
- ^{13}CNMR (100 MHz, chloroform-*d*) δ (ppm): 195,23 (C, C_h); 136,87 (C, C_g); 131,97 (CH, C_e); 129,93 (CH, C_f); 127,63 (C, C_d); 104,13 (C, C_c); 98,16 (C, C_b); -0,02 (CH_3, C_a).
- MS (ESI, *m/z*) calculated for $C_{23}H_{26}OSi_2$: 375,1600 ; found: 375,1590

h) (2,5-dimethoxy-1,4-phenylene)diboronic acid. 3 g of 1,4-dibromo-1,5-dimethoxybenzene (10,14 mmol) were added to 50 ml of anhydrous tetrahydrofuran. The solution was cooled to -78 °C and 13,3 ml of n-butyllithium (21,25 mmol, 2,1 eq., 2,5M in hexane) was added dropwise in 30 min. The mixture was stirred for 5 h at this temperature and 10 ml of triethyl borate (43,4 mmol, 3,4 eq.) was slowly added keeping the

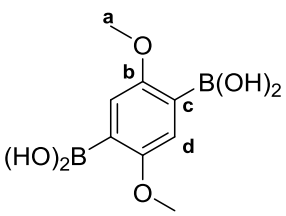

temperature constant. The solution was stirred overnight and warmed slowly to room temperature. The mixture was decomposed with 20 ml of 5% hydrogen chloride and then solvents were removed in vacuum. Obtained product was recrystallized from 100 ml of water/acetonitrile (1:1). Finally 600 mg of white product were obtained (yield: 26 %).

- ^{1}HRMN (300 MHz, DMSO-d_6) δ (ppm): 7,79 (s, 4H, OH); 7,16 (s, 2H, H_d); 3,77 (s, 6H, H_a).
- ^{13}CNMR (100 MHz, DMSO-d_6) δ (ppm): 157,37 (C, C_b); 124,57 (C, C_c); 116,79 (CH, C_d); 55,75 (CH_3, C_a).
- Calculated elemental analysis for $C_8H_{12}B_2O_6$: C 42,55; H 5,36; N 0,00 %. Obtained elemental analysis for $C_8H_{12}B_2O_6$: C 32,9; H 5,92; N <1,6 %.

i) 6,6'-(2,5-dimethoxy-1,4-phenylene)bis(3-bromopyridine). 100 mg of (2,5-dimethoxy-1,4-phenylene)diboronic acid (0,44 mmol), 314,7 mg of 2,5-dibromopiridyn (1,33 mmol, 3 eq.) and 7,5 ml of 2 M sodium carbonate were added to a mixture of toluene/ethanol (4 ml/ 2ml). The mixture was degassed with nitrogen for 1h. Then 51 mg of tetrakis(triphenylphosphine)palladium(0) (0,045 mmol, 0,1 eq.) were added and the mixture was degassed 30 min more. The mixture was heated at 120 °C for 17 h. After cooling the mixture of the reaction to room temperature, it was poured into water and the crude product was extracted with ethyl acetate. The combined organic layers were dried with anhydrous magnesium sulfate. The magnesium sulfate was filtered and the solvents were removed in vacuum. The obtained crude product was purified by silica gel column chromatography using hexane/dichloromethane/diethyl ether (8:2:1) as eluent. 100 mg of yellow solid were obtained as a pure product (yield: 50 %).

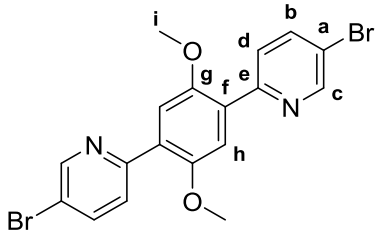

- ^{1}HRMN (300 MHz, Chloroform-*d*) δ (ppm): 8,76 (dd, *J* = 2,4; 0,7 Hz, 2H, H_c); 7,93 (dd, *J* = 8,6; 0,7 Hz, 2H, H_d); 7,84 (dd, *J* = 8,6; 2,4 Hz, 2H, H_b); 7,59 (s, 2H, H_h), 3,92 (s, 6H, H_i).

- ^{13}CNMR (100 MHz, chloroform-*d*) δ (ppm): 153,71 (C, C_a); 151,56 (C, C_g); 150,50 (CH, C_c); 138,52 (CH, C_b); 128,97 (C, C_f); 126,62 (CH, C_d); 119,26 (C, C_a); 114,44 (CH, C_h); 56,43 (CH_3, C_i).
- MS (ESI, *m/z*) calculated for $C_{18}H_{14}O_2N_2Br_2$: 448,9500 ; found: 448,9503
- Calculated elemental analysis for $C_{18}H_{14}O_2N_2Br_2$: C 48,03; H 3,14; N 6,22 %.

  Obtained elemental analysis for $C_{18}H_{14}O_2N_2Br_2$: C 48,93; H 4,06; N 5,60 %.

j) 2,5-bis(5-bromopyridin-2-yl)benzene-1,4-diol. 0,4 g of 6,6'-(2,5-dimethoxy-1,4-phenylene)bis(3-bromopyridine) (0,89 mmol) and 1,18 g of aluminum chloride (8,89 mmol, 10 eq.) were added to 30 ml of toluene and the mixture was stirred for 30 min. The solution was purged with argon and then refluxed for 7h. After cooling the mixture to room temperature it was quenched by slowly addition of water. The crude product was extracted with dichloromethane and the obtained organic phases were dried with anhydrous magnesium sulfate. The magnesium sulfate was filtered and solvents were removed in vacuum. Obtained crude product was purified by silica gel column chromatography using dichloromethane/hexane (7:3) as eluent. 200 mg of yellow solid were obtained as a pure product (yield: 53 %).

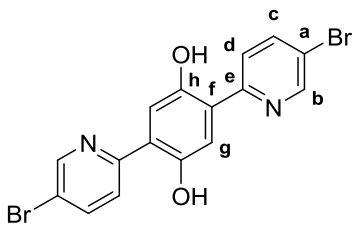

- ^{1}HRMN (300 MHz, Chloroform-*d*) δ (ppm): 8,62 (dd, *J* = 2,4; 0,7 Hz, 2H, H_b); 7,99 (dd, *J* = 8,8; 2,4 Hz, 2H, H_d); 7,83 (m, 2H, H_c); 7,41 (s, 2H, H_g).
- ^{13}CNMR (100 MHz, chloroform-*d*) δ (ppm): 155,53 (CH, C_b); 152,57 (CH, C_c); 151,80 (CH, C_d); 147,67 (C, C_e); 140,75 (C, C_h); 121,41 (C, C_f); 118,78 (CH, C_g); 115,19 (C, C_a).
- MS (ESI, *m/z*) calculated for $C_{16}H_{10}O_2N_2Br_2$: 420,9187 ; found: 420,9183
- Calculated elemental analysis for $C_{16}H_{10}O_2N_2Br_2$: C 45,53; H 2,39; N 6,64 %.

Obtained elemental analysis for $C_{16}H_{10}O_2N_2Br_2$: C 47,73; H 3,81; N 6,40 %.

4.4. SYNTHESIS OF POLYMERS

The same procedure was followed for the synthesis of three polymers:

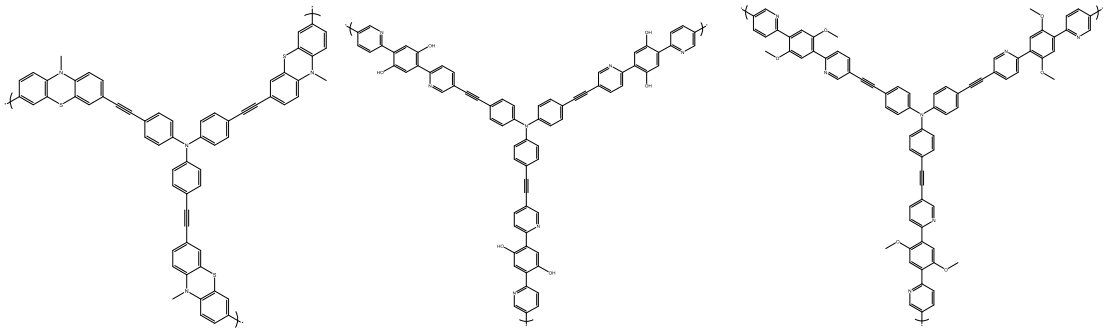

a) POLYMER 7 **b) POLYMER 8** **c) POLYMER 8**

Anhaydrous dimethylformamide was degassed with nitrogen for 30 min. The correspondent monomers (1 eq. /1 eq.) and triethylamine were added to the flask. The mixture was degassed for 1 h more. Then, tetrakis(triphenylphosphine)palladium(0) (0,08 eq.) and copper iodide (0,15 eq.) were added and the mixture was degassed for other 15 min. Finally, the mixture was heated at 80 °C. After 5 days the reaction was stopped and cooled to room temperature. The obtained polymers were purified by Soxhlet extraction, first with dichloromethane (24 h) and then with tetrahydrofuran (24 h). Finally, they were dried in a lyophilizer for 4 days.

a) POLYMER 7

- Yield: % 100
- Calculated elemental analysis: C 79,80 ; H 4,15; N 5,91 %
  Obtained elemental analysis: C 71,60 ; H 6,15; N 4,75 %

b) POLYMER 8

- Yield: % 38 (big amount of the product was lost while drying in the lyophilizer).
- Calculated elemental analysis: C 78,53; H 3,84; N 8,90 %
  Obtained elemental analysis: C 70,55; H 6,56; N 5,48 %

c) POLYMER 9

- Yield: % 95,24
- Calculated elemental analysis: C 79,04; H 4,59; N 8,27 %
  Obtained elemental analysis: C 70,74; H 5,75; N 5,54 %

5. CONCLUSIONS AND FUTURE WORK

In this project three CMPs were synthesized combining a tri-functional redox-active monomer (monomer **1**) and three different dibromine monomers (monomers **4**, **5** and **6**). These CMPs were studied in order to know if their properties could be appropriates for energy storage applications.

In order to confirm that the polymerization occurred, the following techniques were used to characterize the polymers and to study their interesting properties: ^{13}C-NMR (solid), FTIR, elemental analysis, TGA, BET and cyclic voltammetry.

It was determined that using optimized conditions it was possible to obtain conjugated microporous polymers whose specific surface and pore size were adequate to use them as cathode in lithium batteries. Furthermore, it was seen that the electrochemical properties of the free monomers were not lost after the polymerization. This makes the CMPs redox-active and therefore, useful materials for the energy storage devices. Even the three polymers were redox-active, it was seen that polymers **8** and **9** work better in aqueous electrolyte while polymer **7** works better in organic electrolyte. Beside, polymer **9** showed very good results in its textural properties as the specific surface. Therefore, it would be interesting to keep studying more electrochemical properties like the capacity for these materials.

Anyway, it would be interesting also to synthesize more variety of CMPs with the monomers **2** and **3**, and to study how the lack of the redox-activity of these monomers affects in the CMP, because even these monomers are not redox-actives they can provide electronic conduction through the polymer. For that, the synthesis of these monomers will be tried starting for iodide monomers instead of the bromine ones.

KONKLUSIOAK ETA ETORKIZUNEKO LANA

Proiektu honetan hiru CMP sintetizatu dira, erredox aktiboa den monomero trifuntzional bat eta erredox aktibitate desberdineko hiru dibromo monomerotatik abiatuz. CMP hauek aztertuak izan dira energia biltegiratzeko aplikazioetan erabiltzeko propietate egokiak dituzten jakiteko.

Ondorengo metodoak erabili dira polimerizazioak ondo eman diren ikusteko, materialak karakterizatzeko eta hauen propietate interesgarriak aztertzeko: ^{13}C-NMR (solidoa), FTIR, analisis elementala, TGA, BET eta boltametria ziklikoak.

Ikusi da erreakzio baldintza egokiak erabiliz, litiozko baterietan katodo bezala erabiltzeko superfizie espezifiko eta poroen tamaina egokiko materialak sintetizatzea lortu dela. Honetaz gain, ondorioztatu da monomero askeen propietate elektrokimikoak polimerizazioaren ondoren galtzen ez direla. Honek erredox aktibitatea ematen die polimeroei eta ondorioz energia biltegiratzeko gailuetan erabiltzeko material aproposak dira. Nahiz eta hiru polimeroak erredox aktiboak direla ikusi, emaitzak begiratuz ikusi da **8** eta **9** polimeroek elektrolito akuosoan hobe funtzionatzen dutela eta **7** polimeroak berriz, elektrolito organikoan. Gainera, **9** polimeroak oso emaitza interesgarriak erakutsi ditu gainazalaren propietateetan. Ondorioz, pentsatu da material hauen propietate elektrokimikoak aztertzen jarraitu behar dela.

Hala ere, interesgarria izango litzateke CMP desberdin gehiago sintetizatzea monomero **2** eta **3** tik abiatuz. Horrela monomero hauen erredox aktibitate faltak polimeroan duen eragina aztertu ahal izateko. Izan ere, nahiz eta monomero hauek erredox aktiboak ez izan, konduktibitate elektronikoa proportziona dezakete

polimeroan zehar. Horretarako, monomero hauek sintesia egiten saiatuko da ioduro monomerotik abiatuz, bromurotik abiatu ordez.

6. REFERENCES

1. C. Zhang, X. Yang, W. Ren, Y. Wang, F. Su, J.-X. Jiang, *Journal of Power Sources,* 2016, **317**, 49-56.
2. J.M Tarascon, M. Armand, *Nature,* 2001, **414**, 359-367.
3. M. Armand, J.M. Tarascon, *Nature*, 2008, **451**, 652-657.
4. C. Liu, F. Li, L.-P. Ma, H.-M. Cheng, *Advanced Materials*, 2010, **22**, E28-E62.
5. S.Y. Yang, S. Zhang, B.L Fu, Q. Wu, F.L. Liu, C. Deng, *Journal of Solid State Electrochemistry*, 2011, **15**, 2633-2638.
6. N. Casado, D. Mecerreyes, *Revista de plásticos modernos,* 2017, **728**, 19-24.
7. P. Novák, K. Müller, K.S.V. Santhanam, O. Haas, *Chemical Reviews*, 1997, **97**, 207-282.
8. T. Janoschka, M.D. Hager, U.S. Schubert, *Advanced Materials*, 2012, **24**, 6397-6409.
9. R. Garcia, D. Mecerreyes, *Polymer Chemistry*, 2013, **4**, 2206-2214.
10. C.G. Cameron, P.G. Pickup, *Chemical communications*, 1997, **303**.
11. J. Li, K.-H. Ong, P. Sonar, S.-L. Lim, G.-M. Ng, H.-K. Wong, H.-S. Tan, Z.-K. Chen, *Polymer Chemistry*, See DOI: 10.1039/c2py20763j.
12. U. Lange, V.M. Mirsky, *Journal of the Electrochemical Society,* 1990, **137**, 1191.
13. Ester Verde (2014), *Nuevos polímeros porosos como soportes para catalizadores* (Tesis doctoral), Universidad Autónoma de Madrid, Madrid, España.
14. N.Y. Chen, T.F. Degnan, *Chemical Engineering Progress*, 1988, **84**, 32-41.
15. J.N. Armor, *Microporous and Mesoporous Materials,* 1998, **22**, 451-456.
16. A. Corma, H. García, F.X. Llabrés I Xamena, *Chemical Reviews,* 2010, **110**, 4606-4655.
17. S.R. Batten, N.R. Champness, X.M. Chen, J. Garcia-Martinez, S. Kitagawa, L. Öhrström, M. O'Keeffe, M.P. Suh, J. Reedijk, *Pure and Applied Chemistry,* 2013, **85**, 1715-1724.
18. N.B. McKeown, P.M. Budd, *Chemical Society Reviews,* 2006, **35**, 675-683.

19. O.K. Farha, Y.S. Bae, B.G. Hauser, A.M. Spokoyny, R.Q. Snurr, C.A. Mirkin, J.T. Hupp, *Chemical communications,* 2010, **46**, 1056-1058.
20. K.S.W. Sing, D.H. Everett, R.A.W. Haul, L. Moscou, R.A. Pierotti, J. Rouquerol, T. Siemieniewska, *Pure and Applied Chemistry,* 1985, **57**, 603-619.
21. S. Brunauer, P.H. Emmett, E. Teller, *Journal of the American Chemical Society,* 1938, **60**, 309-319.
22. P.M. Budd, B.S. Ghanem, S. Makhseed, N.B. McKeown, K.J. Msayib, C.E. Tattershall, *Chemical Communications,* 2004, **10**, 230-231.
23. A.P. Côté, A.I. Benin, N.W. Ockwig, M. O'Keeffe, A.J. Matzger, O.M. Yaghi, *Science,* 2005, **310**, 1166-1170.
24. V.A. Davankov, M.P. Tsyurupa, *Reactive Polymers,* 1990, **13**, 27-42.
25. J.X. Jiang, F. Su, A. Trewin, C.D. Wood, N.L. Campbell, H. Niu, C. Dickinson, A.Y. Ganin, M.J. Rosseinsky, Y.Z. Khimyak, A.I. Cooper, *Angewandte chemie – International Edition,* 2007, **46**, 8574-8578.
26. R. Chinchilla, Najera, *Chemical Reviews,* 2007, **107**, 874-922.
27. R. Sonogashira, Y. Tohda, N. Hagihara, *Tetrahedron Letters,* 1975, **16**, 4467-4470.
28. S. Zhang, W. Huang, P. Hu, C. Huang, C. Shang, C. Zhang, R. Yang, G. Cui, *Journal of Materials Chemistry A,* 2015, **3**, 1896-1901.
29. C. Zhang, X. Yang, Y. Zhao, W. Wang, M. Yu, J.-X. Jiang, *Polymer*, 2015, **61**, 36-41.
30. R. Dawson, A.I. Cooper, D.J. Adams, *Progress in Polymer Science,* 2012, **37**, 530-563.
31. J.-X. Jiang, A. Trewin, D.J. Adams, A.I. Cooper, *Chemical Science,* 2011, **2**, 1777-1781.
32. Y. Xu, L. Chen, Z. Guo, A. Nagai, D. Jiang, *Journal of the American Chemical Society,* 2011, **133**, 17622-17625.
33. F. Xu, X. Chen, Z. Tang, D. Wu, R. Fu, D. Jiang, *Chemical communications,* 2014, **50**, 4788-4790.
34. Y. Kou, Y. Xu, Z. Guo, D. Jiang, *Angewandte Chemie International Edition,* 2011, **50**, 8753-8757.

35. F. Vilela, K. Zhang, M. Antonietti, *Energy & Environmental Science,* 2012, **5**, 7819-7832.
36. K. Sakaushi, E. Hosono, G. Nickerl, T. Gemming, H. Zhou, S. Kaskel, J. Eckert, *Nature Communications,* 2013, **4**, 1485.
37. K. Sakaushi, E. Hosono, G. Nickerl, H. Zhou, S. Kaskel, J. Eckert, *Journal of Power Sources,* 2014, **245**, 553-556.
38. H. Liao, H. Ding, B. Li, X. Ai, C. Wang, *Journal of Materials Chemistry A,* 2014, **2**, 8854-8858.
39. R.S. Sprick, J.-X. Jiang, B. Bonillo, S. Ren, T. Ratvijitvech, P. Guiglion, M.A. Zwijnenburg, D.J. Adams, A.I. Cooper, *Journal of the American Chemical Society*, 2015, **137**, 3265-3570.
40. J.-X. Jiang, C. Wang, A. Laybourn, T. Hasell, R. Clowes, Y.Z. Khimyak, J. Xiao, S.J. Higgins, D.J. Adams, A.I. Cooper, *Angewandte Chemie International Edition,* 2011, **50**, 1072-1075.
41. J.-X. Jiang, Y. Li, X. Wu, J. Xiao, D.J. Adams, A.I. Cooper, *Macromolecules,* 2013, **46**, 8779-8783.
42. B. Kiskan, M. Antonietti, J. Weber, *Macromolecules*, 2012, **45**, 1356-1361.
43. C. Luo, R. Huang, R. Kevorkyants, M. Pavanello, H. He, C. Wang, *Nano Letters*, 2014, **14**, 1596-1602.
44. S. Zhang, C. Deng, H. Gao, F.L. Meng, M. Zhang, *Electrochimica Acta,* 2012, **107**, 406-412.
45. Z. Song, T. Xu, M.L. Gordin, Y.-B. Jiang, I.-T. Bae, Q. Xiao, H. Zhan, J. Liu, D. Wang, *Nano Letters*, 2012, **12**, 2205-2211.
46. B.L. Ellis, P. Knauth, T. Djenizian, *Advanced Materials*, 2014, **26**, 3368-3397.
47. P.-Z. Li et al., *Angewandte Chemie International Edition,* 2015, **54**, 12746-12750.
48. G.D. Wagh, K.G. Akamanchi, *Tetrahedron Letters*, 2017, **58**, 3032–3036.
49. Z. Chang, Y. Jiang, B. He, J. Chen, Z. Yang, P. Lu, H.S. Kwok, Z. Zhao, H. Qiu, B.Z. Tang, *Chemical communication,* 2013, **49**, 594-596.
50. J.E. McMurry, M.P. Fleming, *Journal of American Chemical Society,* 1974, **96**, 4708-4709.

51. J. Wang, J. Mei, E. Zhao, Z. Song, A. Qin, J.Z. Sun, B.Z. Tang, *Macromolecules,* 2012, **45**, 7692-7703.
52. C.-J. Yang et al., *Journal of Materials Chemistry,* 2012, **22**, 4040-4049.
53. Ch. Wang, M. Kilitziraki, J.A.H. MacBride, I.D.W. Samuel, *Advanced Materials,* 2000, **12**, 217.
54. T. Trefz, Md.K. Kabir, R. Jain, B.O. Patrick, R.G. Hicks, *Canadian Journal of Chemistry,* 2014, **92**, 1010-1020.
55. M. Liras et al., *Journal of Materials Chemistry,* 2016, **4**, 17274-17278.